

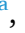











## The $\beta$ -amyloid-induced increased tonic conductance, impaired long-term potentiation and cognitive deficits characteristic of Alzheimer's disease are reversed by an $\alpha 5$ inverse agonist of the GABA type A receptor

Aoife O'Connell <sup>a,1</sup> , Beatriz Calvo-Flores Guzmán <sup>b,1</sup> , Ying Zhai <sup>a</sup> , Cameron N. Keighron <sup>c</sup> , Jordi Boix <sup>d</sup> , Katie Peppercorn <sup>e</sup> , Warren P. Tate <sup>e,f</sup> , Henry J. Waldvogel <sup>b</sup> , Richard LM. Faull <sup>b</sup> , Johanna M. Montgomery <sup>g</sup> , Leo Quinlan <sup>c</sup> , Andrea Kwakowsky <sup>a,b,\*</sup> 

<sup>a</sup> Pharmacology and Therapeutics, School of Pharmacy and Medical Sciences, Institute for Health Discovery and Innovation, Institute for Clinical Trials, Galway Neuroscience Centre, University of Galway, Ireland

<sup>b</sup> Centre for Brain Research, Department of Anatomy and Medical Imaging, Faculty of Medical and Health Sciences, University of Auckland, Auckland, New Zealand

<sup>c</sup> Physiology, School of Pharmacy and Medical Sciences, Galway Neuroscience Centre, University of Galway, Ireland

<sup>d</sup> Centre for Brain Research, Neuro Discovery Behavioural Unit, Faculty of Medical and Health Sciences, University of Auckland, Auckland, New Zealand

<sup>e</sup> Department of Biochemistry, School of Biomedical Sciences, University of Otago, Dunedin, New Zealand

<sup>f</sup> Department of Pathology, Dunedin School of Medicine, University of Otago, Dunedin, New Zealand

<sup>g</sup> Centre for Brain Research, Department of Physiology, Faculty of Medical and Health Sciences, University of Auckland, Auckland, New Zealand

### ARTICLE INFO

#### Keywords:

Alzheimer's disease

GABA

$\alpha 5$ IA

Excitatory/inhibitory balance

### ABSTRACT

Alzheimer's disease is a chronic, progressive neurodegenerative disorder characterized by cognitive impairment, which may arise from disruptions in the excitatory/inhibitory balance within the brain. Gamma-aminobutyric acid (GABA), the principal inhibitory neurotransmitter in the central nervous system, plays a crucial role in maintaining the excitatory/inhibitory balance and regulating neuronal activity involved in memory. In Alzheimer's disease, changes in  $\alpha 5$  GABA A type receptor expression and activity increase tonic inhibition, disturbing the neuronal excitatory/inhibitory balance and ultimately impairing cognitive processes. Therefore, targeting the  $\alpha 5$  GABA A receptor offers a promising therapeutic strategy to mitigate impairments in these processes. This study examined the potential of an  $\alpha 5$  GABA A receptor-selective inverse agonist,  $\alpha 5$ IA, for treating  $\beta$ -amyloid-induced cognitive deficits and the underlying mechanism of action, using *ex vivo* micro-electrode array and patch clamp electrophysiology. The inverse agonist,  $\alpha 5$ IA, improved impaired long-term potentiation, reduced elevated tonic conductance in CA1 hippocampal neurons and improved long-term spatial memory deficits induced by  $\beta$ -amyloid. These findings highlight  $\alpha 5$ IA's ability to restore excitatory/inhibitory balance and, thereby, cognitive function. The selective targeting of  $\alpha 5$  GABA type A receptors with  $\alpha 5$  GABA A receptor inverse agonists, such as  $\alpha 5$ IA, represents a promising direction for developing novel Alzheimer's disease therapies.

### 1. Introduction

Alzheimer's disease (AD) is a chronic, progressive neurodegenerative disorder with clinical symptoms including diminished memory and cognitive function. It is the most prevalent cause of dementia, accounting for 60-80% of dementia cases (Alzheimer's disease facts and figures, 2023). The burden of this severely debilitating disease is apparent, with AD and other dementias among the top 10 causes of

death globally (World Health Organisation, 2020). The characteristic hallmarks of AD include brain shrinkage, accumulation of  $\beta$ -amyloid ( $A\beta$ ) plaques, and neurofibrillary tangles (NFT) composed of hyperphosphorylated tau (Soria Lopez et al., 2019). AD is also characterized by a significantly disturbed excitatory/inhibitory (E/I) balance in the brain, which may be a critical factor underlying the cognitive deficits characteristic of the disease (Francis, 2005; Vinnakota et al., 2020; Govindpani et al., 2017). To date, research has focused on targeting the

\* Corresponding author. Pharmacology and Therapeutics, School of Medicine, Galway Neuroscience Centre, University of Galway, Ireland.

E-mail address: [andrea.kwakowsky@universityofgalway.ie](mailto:andrea.kwakowsky@universityofgalway.ie) (A. Kwakowsky).

<sup>1</sup> These authors contributed equally to this work.

excitatory portion of the E/I imbalance, with most AD drugs approved by the US Food and Drug Administration targeting the cholinergic and glutamatergic neurotransmitter systems. Nevertheless, the symptomatic relief provided by these therapies is only marginal, and the progression or underlying causes of the disease are not addressed (Vinnakota et al., 2020). Given the ever-increasing burden of AD, the urgent need for the identification of novel targets for the development of disease-modifying therapeutic agents is clear.

It has been well documented that A $\beta$  induces neurotoxicity via an excitotoxic pathway, including glutamate accumulation and N-methyl-D-aspartate (NMDA) overactivation (Koh and Choi, 1991; Wu et al., 1995; Harkany et al., 2000). A hypothesis that has emerged in recent years shifts the focus to the inhibitory side of the E/I imbalance, suggesting that by targeting gamma-aminobutyric acid (GABA) neurotransmission, neuronal vulnerability to excitotoxic damage and, ultimately, neuronal death could be reduced (Govindpani et al., 2017). Current evidence indicates that the GABAergic system undergoes significant remodeling in AD, with GABA, GABA transporters, GABA-related enzymes, and GABA receptors among the components most affected (Govindpani et al., 2017; Carello-Collar et al., 2023; Bi et al., 2020; Kwakowsky et al., 2018a; Xu et al., 2020; Palop and Mucke, 2016; Rissman and Mobley, 2011; Li et al., 2016; Rissman et al., 2007). These changes likely reflect the reorganization of neuronal circuits to maintain a stable neuronal network rather than simple compensatory mechanisms alone (Kwakowsky et al., 2018b). GABA is the most prominent inhibitory neurotransmitter in the central nervous system and plays a central role in maintaining the E/I balance and regulating neuronal activity involved in memory function (Paulsen and Moser, 1998). As a result, it has been postulated that AD-induced changes in this system are responsible for some of the symptoms characteristic of AD (Jiménez-Balado and Eich, 2021; Wu et al., 2014a; Calvo-Flores Guzman et al., 2020a; Jo et al., 2014).

On a molecular level, it has been proposed that deficits in mitochondrial adenosine triphosphate (ATP), which occur during ageing, can activate the glutamate decarboxylase (GAD) enzyme, resulting in increased GABA synthesis and release (Madl and Royer, 2000). An alternative theory suggests that GABA production by reactive astrocytes, which are increased in AD models, increases extracellular GABA (Alia and Roßner, 2018). In both cases, increased extracellular GABA would activate extrasynaptic GABA receptors. GABA type A receptors (GABAARs) are involved in many important physiological brain functions. Subunit  $\alpha$ 5-containing GABAARs ( $\alpha$ 5-GABAARs) are of particular interest in AD given their high expression in the hippocampus, where they account for over 25% of GABAARs, and contribute to tonic inhibition (Olsen and Sieghart, 2009; Lee and Maguire, 2014). The maintenance of physiological  $\alpha$ 5-GABAAR expression and activity is crucial for learning and memory processes. Both *in vitro* and *in vivo* evidence support this;  $\alpha$ 5-GABAAR knock-out or point mutant mice display enhanced spatial memory and improved associative learning (Crestani et al., 2002; Collinson et al., 2002). In a genetic model of AD (5xFAD mice),  $\alpha$ 5-GABAARs were reportedly upregulated in the dentate gyrus, leading to increased tonic inhibition and impaired spatial memory (Wu et al., 2014b). Additionally, our laboratory has previously shown in an A $\beta$ -injected mouse model, tonic inhibition was increased in CA1 pyramidal neurons (Calvo-Flores Guzman et al., 2020a). Earlier work found that  $\alpha$ 5-GABAAR expression and function were largely unchanged in AD patients (Howell et al., 2000); however, more recent work from our laboratory reports increased levels of  $\alpha$ 5-GABAARs in the CA1 hippocampal subregion of the human AD brain (Kwakowsky et al., 2018a), and we found A $\beta$  application upregulated  $\alpha$ 5-GABAAR expression in mouse primary neuronal cultures (Vinnakota et al., 2020). AD-induced changes in  $\alpha$ 5-GABAAR expression and activity increase tonic inhibition, disrupting the neuronal E/I balance and ultimately have detrimental effects on cognitive function and processes such as learning and memory (Vinnakota et al., 2020; Calvo-Flores Guzman et al., 2020a; Kwakowsky et al., 2021). Hence, targeting  $\alpha$ 5-GABAAR using an

appropriate compound represents a compelling avenue for the beneficial treatment of AD (Kwakowsky et al., 2021; Calvo-Flores Guzman et al., 2018).

Based on the high expression of  $\alpha$ 5-GABAARs and their strong involvement in learning, memory and cognitive processes, it was hypothesized that  $\alpha$ 5-GABAAR antagonists and/or inverse agonists could enhance hippocampally mediated cognitive functions.  $\alpha$ 5-GABAAR inverse agonists and negative allosteric modulators (NAMs) were of particular interest as they have no convulsant or anxiogenic side effects when examined *in vivo* using wild-type or rodent models of Down syndrome, neuronal excitotoxicity or diazepam-induced memory impairment (Martin et al., 2009; Atack, 2010; Braudeau et al., 2011a; Chambers et al., 2004; Kawaharada et al., 2018; Hipp et al., 2021). Recent studies have validated this theory;  $\alpha$ 5-GABAAR inverse agonists or NAMs have been shown to reduce tonic inhibition (Manzo et al., 2021; Nuwer et al., 2023) and enhance long-term potentiation (LTP) *in vitro* and *ex vivo* (Kawaharada et al., 2018; Dawson et al., 2006). *In vivo*,  $\alpha$ 5-GABAAR inverse agonist or NAM treatment has been reported to improve cognitive functions in wild-type rodents and rodent models of memory impairment (Martin et al., 2009; Braudeau et al., 2011a, 2011b; Chambers et al., 2004; Kawaharada et al., 2018; Hipp et al., 2021; Dawson et al., 2006; Yuan et al., 2021; Collinson et al., 2006), in wild-type non-human primates, and in humans with ethanol-induced memory impairments (Atack, 2010; Hipp et al., 2021; Nutt et al., 2007).  $\alpha$ 5-GABAAR NAMs' effects in AD models have also been investigated with RY-080, an  $\alpha$ 5-GABAAR NAM, showing reduced AD-associated psychomotor agitation in a rTg4510 mouse model of AD (Xu et al., 2018). Importantly,  $\alpha$ 5-GABAAR positive allosteric modulators (PAMs) also display favorable cognitive effects, with PAM treatment improving memory in aged rats with cognitive impairment (Koh et al., 2013) and acute and chronic treatment improving working memory in a 5xFAD model of AD (Bernardo et al., 2025). While these results suggest a beneficial role for targeting  $\alpha$ 5-GABAARs in AD, the results of  $\alpha$ 5-GABAAR modulation appears more complex and context-dependent. Specifically, Petrache et al. (2020) reported that an  $\alpha$ 5-GABAAR NAM exacerbated aberrant inhibition in the  $APP^{NL-F/NL-F}$  model of AD, while Arandelović et al. (2022) reported that  $\alpha$ 5-GABAAR PAMs and NAMs failed to display favorable behavioral effects in the 5xFAD model of AD. However, AD-induced cognitive symptoms had not fully developed in these animals at the time of treatment.

The compound 3-(5-methylisoxazol-3-yl)-6-[(1-methyl-1,2,3-triazol-4-yl)methoxy]-1,2,4-triazolo [3,4-a]phthalazine ( $\alpha$ 5IA) is an  $\alpha$ 5-GABAAR-selective inverse agonist with well-characterized *in vitro* and *in vivo* pharmacological properties (Atack, 2010; Dawson et al., 2006).  $\alpha$ 5IA is highly selective for the benzodiazepine  $\alpha$ 1/ $\alpha$ 2/ $\alpha$ 3 and  $\alpha$ 5-GABAAR binding site with equivalent sub-nanomolar affinity and shows  $\alpha$ 5-GABAAR selective efficacy. The plasma drug concentration required to reach 50% occupancy in humans is 10 ng/ml with a half-life of 2-2.5 h (Atack, 2008, 2010; Eng et al., 2010).  $\alpha$ 5IA has a short plasma life in rodents (0.6-0.9 h), but receptor occupancy was sustained, varying only from 74% to 87% within the time period of 0.5-20 h post dose (Atack et al., 2009a).  $\alpha$ 5IA significantly enhances LTP and cognition in wild-type mice without major side effects such as anxiety, convulsions, seizures or alterations in motor functions (Dawson et al., 2006; Atack et al., 2009b). The potential of  $\alpha$ 5IA for cognitive improvement has been tested in various disease models; for example, in genetic mouse models of Down syndrome,  $\alpha$ 5IA improved learning and memory outcomes (Braudeau et al., 2011b, 2011a; Duchon et al., 2020), and in healthy human adolescents,  $\alpha$ 5IA attenuated ethanol-induced word recall impairments (Nutt et al., 2007). These *in vivo* studies confirm the key role of  $\alpha$ 5-GABAARs in cognitive and memory processes while highlighting the potential for  $\alpha$ 5IA to enhance cognition in various disorders. Despite this strong evidence, few studies have investigated  $\alpha$ 5IA's potential benefit in chronic neurodegenerative disorders such as AD, with current studies providing only preliminary support for the use of  $\alpha$ 5IA in the treatment of AD. We previously examined  $\alpha$ 5IA's effects on

primary hippocampal cultures treated with A $\beta$  (Vinnakota et al., 2020). The treatment prevented A $\beta$ -induced cell loss and reversed A $\beta$ -induced changes in  $\alpha$ 5-GABAAR expression, highlighting the potential of  $\alpha$ 5IA for the treatment of AD. This study aimed to enhance this preclinical evidence by examining the  $\alpha$ 5IA's potential to ameliorate A $\beta$ -induced cognitive deficits *in vivo* and by exploring the underlying electrophysiological mechanism using *ex vivo* brain slices.

## 2. Methods

### 2.1. $\beta$ -amyloid 1-42 preparation

$\beta$ -amyloid 1-42 (A $\beta$ <sub>1-42</sub>) preparation has previously been described by Calvo-Flores Guzman et al. (Calvo-Flores Guzman et al., 2020a) and Yeung et al. (Yeung et al., 2020). Briefly, A $\beta$ <sub>1-42</sub> was produced as a recombinant protein which has a maltose-binding protein (MBP) with a proteolytic cleavage site for Factor X separating both segments. The solubilizing character of the MBP ensures high protein expression in *Escherichia coli* (Kapust and Waugh, 1999). Following the expression of the recombinant protein, the product was purified using an amylose column to which the MBP segment binds. The fusion protein is eluted from the resin using maltose and then concentrated by ammonium sulfate precipitation. After cleavage by Factor X, the released A $\beta$ <sub>1-42</sub> was isolated and further purified using fast protein liquid hydrophobic chromatography in 0–50% v/v acetonitrile/0.1% v/v trifluoroacetic acid (TFA). Fractions containing pure A $\beta$ <sub>1-42</sub> were detected immunologically using antibodies against residues 17–24 of A $\beta$ <sub>1-42</sub>. These fractions were then lyophilized to remove the solvent. The expected molecular ion for the desired product was confirmed using mass spectrometry. A bicinchoninic acid assay (BCA) at 60 °C for 30 min was used to determine the concentration of the protein fragment. Before use, the prepared monomer was diluted in aCSF (147 mM Na<sup>+</sup>, 3.5 mM K<sup>+</sup>, 2 mM Ca<sup>2+</sup>, 1 mM Mg<sup>2+</sup> [pH 7.3]), and the solution was aged at 37 °C for 48 h. This facilitated the formation of A $\beta$  aggregates, which were confirmed by SDS-PAGE and native-PAGE. For the microelectrode array experiment, Ab1-42 was sourced from GenicBio (HA-42-T-20) and aggregated as described here.

### 2.2. *Ex vivo* Alzheimer's disease model experiments

#### 2.2.1. Brain slice preparation

All experiments were approved and performed within the regulations of the University of Galway Animal Care and Research Ethics Committee (approval number: 2022.10.002). For microelectrode array experiments, adult (4-8-month-old) male and female C57BL/6J mice were housed at the University of Galway. Animals were pair-housed with food and water supplied *ad libitum*. The animal holding room was maintained at a constant temperature of 21 ± 2 °C and intervals of 45–55% humidity on a 12-h light/dark cycle.

C57BL/6J mice of both sexes were euthanized by cervical dislocation. Brains were quickly removed and placed in a vibratome chamber (VT1200S, Leica Microsystems, Germany), filled with ice-cold 'slicing' artificial cerebrospinal fluid (aCSF) solution (105 mM Sucrose, 25 mM D-(+)-Glucose, 125 mM NaCl, 25 mM NaHCO<sub>3</sub>, 2.5 mM KCl, 1.25 mM NaH<sub>2</sub>PO<sub>4</sub>·H<sub>2</sub>O, 7 mM MgCl<sub>2</sub>·6H<sub>2</sub>O and 0.5 mM CaCl<sub>2</sub>·2H<sub>2</sub>O) constantly saturated with 95% O<sub>2</sub>/5% CO<sub>2</sub>. Brain slices (250  $\mu$ m) containing the hippocampus were cut coronally using a vibratome. Slices were placed in a recovery chamber containing oxygenated aCSF (125 mM NaCl, 25 mM D-(+)-Glucose, 25 mM NaHCO<sub>3</sub>, 2.5 mM KCl, 1.25 mM NaH<sub>2</sub>PO<sub>4</sub>·H<sub>2</sub>O, 1 mM MgCl<sub>2</sub>·6H<sub>2</sub>O and 2 mM CaCl<sub>2</sub>·2H<sub>2</sub>O) for at least 1 h.

#### 2.2.2. Drug treatments

A total of 31 brain slices containing the hippocampus were prepared with treatment groups as follows: aCSF (n = 5-8 slices), 100 nM A $\beta$ <sub>1-42</sub> (n = 5-7 slices), 100 nM A $\beta$ <sub>1-42</sub> & 1  $\mu$ M  $\alpha$ 5IA (n = 5-10 slices) and 1  $\mu$ M  $\alpha$ 5IA (n = 6-9 slices). Aggregated A $\beta$ <sub>1-42</sub> and/or  $\alpha$ 5IA were added to the

recovery chamber, and brain slices were treated for 1h.

**2.2.2.1. Microelectrode array recordings.** Slices were transferred to a microelectrode array (MEA) chip (60MEA200/30iR-Ti, Multichannel Systems, Germany) and constantly perfused with oxygenated aCSF maintained at 32 °C. Slices were positioned using an inverted microscope (LPlan 4x/0.13, Optika IM-3 Inverted Routine Microscope) so that most of the electrodes were in contact with the hippocampal region. A titanium slice anchor with nylon mesh was placed on top of the slice to prevent displacement, and an image was captured. Perfusion aCSF, constantly bubbled with 95% O<sub>2</sub>/5% CO<sub>2</sub>, was delivered at an inflow rate of 2 ml/min and outflow of 2.5 ml/min. After positioning, slices were allowed to recover for 15-20 min, following which, field excitatory postsynaptic potentials (fEPSPs) were recorded using a MEA2100 system (Multichannel Systems, Germany). Only responses with fEPSPs latencies  $\geq$  3 ms following stimulation were analysed to ensure postsynaptic origin. All recordings were conducted using the Multichannel Experimenter Software (version 2.20.9.23272). Data were digitized and expressed at 20 kHz. Amplitude, duration and frequency of stimulation were controlled by Multichannel Experimenter. Stimulations were applied using a stimulating electrode along the pyramidal layer of the CA1 region, one recording electrode was chosen along the pyramidal or radiatum layer of the CA1 region. MEA recordings were analysed using Multichannel Analyzer (version 2.20.9.23272).

For input-output recordings, biphasic rectangular pulses (200  $\mu$ s in duration – 100 $\mu$ s positive, 100 $\mu$ s negative) were applied using a stimulating electrode along the pyramidal layer of the CA1 subregion. Input voltages from 0.5 to 5V were applied, and the fEPSP amplitudes and slopes were recorded. Recording electrodes on the pyramidal layer and stratum radiatum were chosen based on the shape of the fEPSP response. The 20-80% slope of the initial descending phase of the fEPSP was measured as an index of synaptic strength. The input/output curve informed the stimulation intensity; an intensity which produced 40-60% of the maximum response was chosen for all other stimulation protocols.

Paired-pulse facilitation (PPF) was examined as a measure of short-term plasticity. Two biphasic rectangular stimuli were given 20 ms apart. This was repeated 3 times. The PPF ratio was calculated, and data analysis was performed using the Multichannel Analyser and Excel.

Long-term potentiation (LTP) was examined as a measure of long-term plasticity. Baseline stimulation consisted of one biphasic rectangular stimulus delivered at 1-min intervals for 30 min. A Theta Burst Stimulation (TBS) protocol was used for LTP induction (Abrahamsson et al., 2016). Recording continued for 90 min following TBS induction. fEPSP amplitudes were measured, and data analysis was performed using the Multichannel Analyser and Excel.

### 2.3. *In vivo* Alzheimer's disease model experiments

#### 2.3.1. Animals

All experiments were approved and performed within the regulations of the University of Auckland Animal Ethics Committee (approval numbers: 001586 and 001655). C57BL/6J mice were housed at the University of Auckland, Vernon Jensen Unit for behavioural, patch clamp and immunohistochemistry experiments. Animals were group-housed with food and water supplied *ad libitum*. The animal holding room was maintained at a constant temperature of 21 ± 2 °C and intervals of 45–55% humidity on a 12-h light/dark cycle.

For whole-cell patch-clamp experiments, 20 male C57BL/6J mice (2-month-old) were euthanized 7 days post A $\beta$ <sub>1-42</sub> injection. For behavioral and immunohistochemistry experiments, 100 male C57BL/6J mice (18-month-old) were utilized and after euthanasia, tissue collection was performed for further immunohistochemistry (Fig. 1). Treatment groups were as follows; Naïve control, no treatment (n = 14 animals), ACSF stereotaxic injection (n = 14 animals), Scrambled A $\beta$ <sub>1-42</sub> stereotaxic injection (n = 14 animals), A $\beta$ <sub>1-42</sub> stereotaxic injection (n = 14 animals),

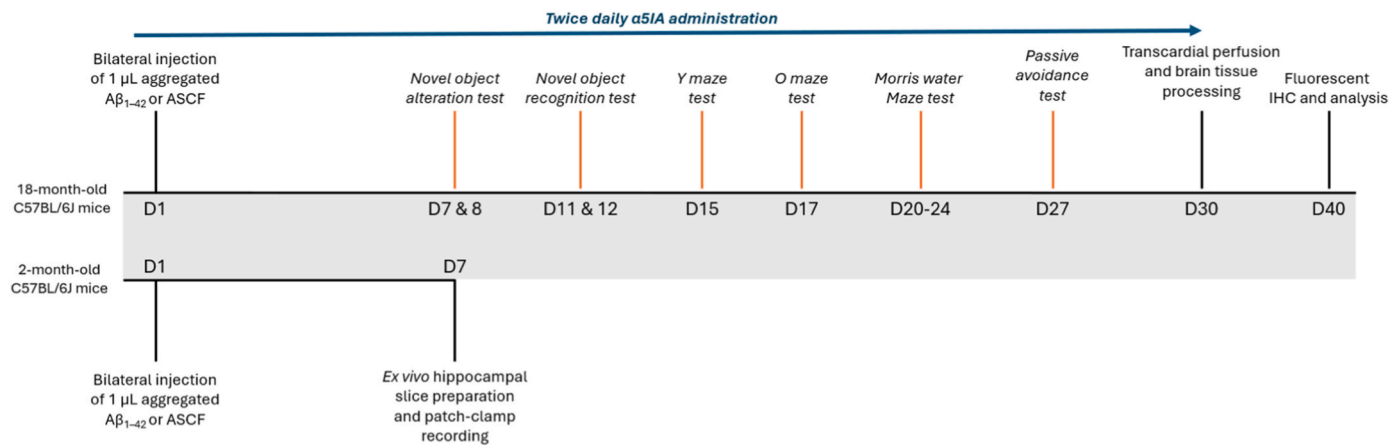


**Fig. 1.** *In vivo* Alzheimer's disease model experimental timeline. Overview of the experimental timeline for all *in vivo* Alzheimer's disease model experiments.  $\beta$ -amyloid ( $A\beta$ ) stereotaxic injection was performed on day 1. A subgroup of animals received twice daily  $\alpha 5IA$  administration for the following 30 days. On day 7, acute hippocampal slices were prepared and patch clamp recordings performed. On another group of aged mice behavioral testing was performed between day 7 and day 27. On day 30, the animals were euthanized, and the tissue was processed. Fluorescent immunohistochemistry (IHC) was performed on the brain tissue, and images were obtained and analyzed.

$A\beta_{1-42}$  stereotaxic injection +  $\alpha 5IA$  (1 mg/kg) ( $n = 14$  animals),  $A\beta_{1-42}$  stereotaxic injection +  $\alpha 5IA$  (5 mg/kg,  $n = 14$  animals) and  $A\beta_{1-42}$  stereotaxic injection + vehicle (0.5% methyl cellulose,  $n = 14$  animals).  $\alpha 5IA$  (1 mg/kg or 5 mg/kg) was administered intraperitoneally, twice daily (9 a.m. and 9 p.m.) for 30 days. The dose and dosing regimen were chosen based on prior  $\alpha 5IA$  *in vivo* studies to allow stable receptor occupancy and effect (Atack, 2008, 2010; Dawson et al., 2006; Collinson et al., 2006; Braudeau et al., 2011b).

### 2.3.2. Stereotaxic injection

Prior to surgery mice were anesthetized by subcutaneous injection of 1 mg/kg medetomidine and 75 mg/kg ketamine, as per the Institutional Drug Administration Order (IDAO: 001586/3 and 001655/3). Bilateral hippocampal stereotaxic surgery was performed, with coordinates for injection at three depths determined relative to the bregma (anterior-posterior,  $-2.0$  mm; medial-lateral,  $\pm 1.3$  mm; dorsal-ventral,  $-1.9$ ,  $2.4$ , and  $2.9$  mm) with  $1 \mu L$   $20 \mu M$  aggregated  $A\beta_{1-42}$  or ACSF injected at  $0.1 \mu L/min$  ( $0.33 \mu L$  per dorso-ventral coordinate) (Calvo-Flores Guzman et al., 2020a; Yeung et al., 2020; Kwakowsky et al., 2016a). Following surgery, anesthesia was reversed via subcutaneous administration of 1 mg/kg atipamezole, and 5 mg/kg carprofen, as per the Institutional Drug Administration Order (IDAO: 001586/1&2 and 001655/1&2). Animal health and well-being were closely monitored during the experiment. Naïve control (NC) animals did not undergo any surgical procedures.

### 2.3.3. Ex vivo whole-cell voltage-clamp recording

**2.3.3.1. Brain slice preparation.** Two-month-old naïve control, aCSF-injected, and  $A\beta_{1-42}$ -injected mice ( $n = 20$  animals) groups were euthanized by cervical dislocation 7 days post-injection. Brains were quickly removed and placed in an ice-cold patch-clamp slicing aCSF solution (93 mM N-methyl-D-glucamine (NMDG), 93 mM KCl, 1.2 mM  $NaH_2PO_4$ , 30 mM  $NaHCO_3$ , 20 mM HEPES, 25 mM D-glucose, 5 mM sodium ascorbate, 2 mM thiourea, 3 mM sodium pyruvate, 10 mM  $MgSO_4$  and 0.5 mM  $CaCl_2$ , pH 7.35). Slices ( $350 \mu m$ ) were cut using a vibratome (Leica VT 12000, Wetzlar, Germany). The slices were incubated in a chamber (GD100, Grant, Cambridge, UK) containing patch-clamp slicing aCSF at  $34^\circ C$  for 12 min before being transferred and stored for recovery at  $21^\circ C$  in a holding chamber in aCSF patch-clamp recording solution (97 mM NaCl, 2.5 mM KCl, 1.2 mM  $NaH_2PO_4$ , 30 mM  $NaHCO_3$ , 20 mM HEPES, 25 mM D-glucose, 5 mM sodium ascorbate, 2 mM thiourea, 3 mM sodium pyruvate, 2 mM  $MgSO_4$  and 2 mM  $CaCl_2$ , pH

7.35), in the presence of 3 mM kynurenic acid and 5  $\mu M$  GABA.

**2.3.3.2. Whole-cell patch-clamp recording.** Whole-cell patch-clamp recordings were performed as described in Calvo-Flores Guzman et al. (2020a). Briefly, under IR-DIC optics (Olympus TH4-200, BX51WI, Tokyo, Japan) equipped with a video camera (CCD, C7500-51, S. No 6  $\times$  0047; Hamamatsu, Hamamatsu, Japan) CA1 pyramidal cells were visualized. A MultiClamp 700B amplifier (Axon Instruments, San Jose, CA, USA) was used to perform voltage-clamp recordings. Slices were continually perfused with a patch-clamp recording aCSF solution containing 3 mM kynurenic acid and 5  $\mu M$  GABA, which was constantly saturated with 95%  $O_2/5\%$   $CO_2$  and maintained at  $32^\circ C$ . Kynurenic acid was added to block ionotropic glutamate receptors, and GABA was added to increase ambient GABA levels and facilitate tonic conductance measurement. Tetrodotoxin (TTX) (1078, Tocris, Bristol, UK) at 5  $\mu M$  and  $CdCl_2$  (202908, Sigma Aldrich) at 50  $\mu M$  were used to block voltage-gated  $Na^+$  and  $Ca^{2+}$  channels, respectively. The GABA receptor antagonist bicuculline methiodate (BMI) was used at 100  $\mu M$  to measure tonic conductance.

A dual-stage glass micropipette puller PC-10 (Narishige, Tokyo, Japan) was used to create glass microelectrodes with a resistance of 3–5  $M\Omega$ , which were filled with internal solution (140 mM CsCl, 1 mM  $MgCl_2$ , 10 mM HEPES, 0.1 mM EGTA, 4 mM NaCl, 2 mM MgATP and 0.3 mM NaGTP, pH 7.28, osmolarity,  $\sim 280$  mOsm). Neurons were held at  $-70$  mV in voltage-clamp configuration. If the series resistance altered more than 30% during a recording, the recording would be discarded. Following a 5-min stable baseline recording in aCSF with or without  $\alpha 5IA$ , BMI was perfused and tonic conductance was recorded from acute hippocampal slices. Average series resistance was 21  $M\Omega$  in slices from naïve control mice, 18  $M\Omega$  in slices from  $A\beta_{1-42}$ -injected mice and 19  $M\Omega$  in slices from aCSF-injected mice and slices from  $A\beta_{1-42}$ -injected mice acutely treated *ex vivo* with  $\alpha 5IA$ . Recordings were sampled at 10 kHz, low-pass filtered at 3 kHz and digitalized using an Axon Digidata 1550B plus HumSilencer apparatus (Axon Instruments, San Jose, CA, USA and SDR Scientific, Sydney, NSW, Australia).

**2.3.3.3. Tonic current measurements in hippocampal slices.** Measurement of tonic conductance was performed as described in (Calvo-Flores Guzman et al., 2020a) and Glykys and Mody (2006). Briefly, a shift in the holding current caused by the addition of BMI was used to measure tonic current. All-point histograms were generated for control and BMI-periods, and a Gaussian curve was fit to the data. By subtracting the mean current value for the control period from the mean current value

for the BMI period, tonic inhibition was determined. For  $\alpha 5IA$ -treated slices 100 nM of  $\alpha 5IA$  was added to the patch-clamp recording aCSF solution, and a measurement of tonic conductance was obtained.

### 2.3.4. Immunohistochemistry

**2.3.4.1. Mouse brain tissue preparation.** Thirty days post  $A\beta$ -injection, mice were deeply anaesthetized with 75 mg/kg ketamine and 1 mg/kg dormitor and transcardially perfused with 4% paraformaldehyde (PFA). Their brains were extracted and quickly fixed in 4% PFA. Hippocampal coronal sections (30  $\mu$ m) were cut on a freezing microtome (Microm Ginbit, Walldorf, Germany) and collected in tris buffered saline (TBS) solution.

**2.3.4.2. Free-floating fluorescence immunohistochemistry.** Free-floating fluorescence immunohistochemistry (Ff-IHC) was performed using the method described by Kwakowsky et al. (Kwakowsky et al., 2016a). Briefly, hippocampal sections were washed three times in TBS and incubated in 0.05M TBS/0.3% Triton (TTB) with 0.25% BSA and 1% goat serum. The sections were then incubated with primary antibodies diluted in TTB for 72 h at 4 °C. Immunolabeling was performed with primary antibodies against NeuN (neuronal nuclear marker; 1:1000, Millipore, monoclonal mouse, MAB377). Then, following three washes in TBS, the sections were incubated in Alexa Fluor secondary antibody (goat anti-mouse Alexa Fluor 488 (1:500, Invitrogen, A11029, RRID: AB\_138404)) and finally, in Hoechst (1/10,000 in TTB, Invitrogen) nuclear counterstain.

**2.3.4.3. Imaging and quantification.** To assess the extent of pyramidal cell loss in the stratum pyramidale of the CA1 region, the number of NeuN-positive pyramidal neurons was counted in a 10,296  $\mu$ m<sup>2</sup> area of the stratum pyramidale of the CA1 region, as earlier reported (Calvo-Flores Guzman et al., 2020b). Sections in which the needle track was identifiable were selected for analysis. Two sections were used for counting per animal, and the average of these neuronal counts was used as a representative number of neurons per region of interest per animal (n = 8 animals per treatment group). Sections with NeuN labeling were examined under a Zeiss LSM 710 inverted confocal laser-scanning microscope (Carl Zeiss, Jena, Germany).

### 2.3.5. Behavioral testing

The cognitive performance of the mice was analysed using behavioral tests that target different types of hippocampal-dependent memories, including long-term memory (novel object alteration (NOAL), novel object recognition (NOR) and the Morris water maze (MWM)), short-term spatial memory (Y-maze test (YM)), and non-spatial memory (passive avoidance test). Finally, the O-maze test was used to measure the anxiety levels of the mice. Animals received the  $\alpha 5IA$  injections at 9 a.m., and behavioural tests were conducted approximately 1-2 h later. The NOAL test was performed on post-injection day 7-8, the NOR test was performed on post-injection day 11-12, the Y-maze test was performed on post-injection day 15, the O-maze test was performed on post-injection day 17, the MWM on post-injection day 20, and the passive avoidance test on post-injection day 27. The tracking image analyzer system EthoVision XT 9 (Noldus; Wageningen, Netherlands) was used to analyze behavioral data, except for determining the time spent near objects in NOAL and NOR. These measurements were taken using manual stopwatches.

**2.3.5.1. Novel object alteration test.** Each mouse was placed in a square arena (25 cm  $\times$  29 cm  $\times$  25 cm) with non-transparent plexiglass walls and given 10 min for habituation. Two identical objects were then placed in the area at a predefined location, and the mice were allowed to interact and explore the objects for 5 min. Twenty-four hours later, the process was repeated. However, one of the objects was placed in a new

location; animals were allowed to interact and explore the objects for 5 min. No minimum exploration time was applied, and all data was included in analysis. The following discrimination ratio was used:

$$\frac{\text{time near the object at new position} - \text{time near the object at old position}}{\text{time near the object at new position} + \text{time near the object at old position}}$$

**2.3.5.2. Novel object recognition test.** The NOR test was performed in the same arena as the NOAL test, and each mouse was given 10 min for habituation. Two identical objects were then placed in the area at a predefined location and the mice were allowed to interact and explore the objects for 5 min. Twenty-four hours later, the process was repeated, however, now with one novel object; again, they were allowed to interact and explore the objects for 5 min. Time spent exploring the novel object is considered an index of recognition memory. No minimum exploration time was applied, and all data was included in analysis. The following discrimination ratio for a novel over a familiar object was used (Yeung et al., 2020; Kwakowsky et al., 2016b):

$$\frac{\text{time near the new object} - \text{time near the old object}}{\text{time near the new object} + \text{time near the old object}}$$

**2.3.5.3. Y-maze test.** The apparatus used for the YM study was constructed out of plexiglass with the three arms of the maze positioned at a 120° angle relative to each other. Each arm is identical (52 cm  $\times$  12.5 cm); however, different spatial cues are placed in each arm. The start arm for each experiment was chosen randomly: each mouse was placed in the YM environment on two occasions that were separated by a 2-min interval. During the first 5-min trial, one of the three arms was randomly blocked. In the second trial, all the arms were opened for exploration; the total amount of time the mouse took to explore each arm was recorded for 3 min. During the inter-trial interval (2 min), the animal was returned to its home cage and the maze was cleaned. The alternation percentage was calculated as the percentage of the ratio of actual to possible alternations. An index of the time spent in the new previously unexplored arm as opposed to the familiar explored arm was used to assess any behavioral differences between each group, and was calculated as follows:

$$\frac{\text{time spent in new arm} - \text{time spent in old arm}}{\text{time spent in new arm} + \text{time spent in old arm}}$$

**2.3.5.4. O-maze test.** The O-maze apparatus consisted of a circular maze (40 cm diameter) with two protected (closed) arms, where the mice usually feel safer, and two unprotected (open) arms where increased time in the closed arm is indicative of anxiety-like behavior. Each mouse was randomly placed in one of the closed arms. The recording was performed under red light conditions over 5 min. The total time spent by each mouse in the closed and open arms was measured. Anxiety-like behavior was estimated based on the total time spent in the closed arms of the apparatus.

**2.3.5.5. Morris water maze test.** The MWM test was used to evaluate long-term spatial memory. The MWM apparatus comprises a circular black tank (diameter, 130 cm; height, 130 cm) filled with tap water (maintained at 20 °C), with a circular escape platform (10 cm diameter) and several navigation cues to provide spatial orientation for the mice. Each test was recorded via a video camera suspended from the ceiling. The mouse's starting position was randomly assigned, however, the location of the hidden platform was kept constant. If a mouse did not successfully find the platform within 90 s, it was placed on the platform for 10 s before being returned to its cage. For four days, the mice underwent four repeat trials per day, between which they were dried with a towel, placed in their cage and kept over a heating blanket for 10 min. The latency period before the mouse reached the platform was measured.

**2.3.5.6. Passive avoidance test.** The passive avoidance test apparatus consisted of a two-compartment box, with one bright and one dark compartment (16 cm × 18 cm). During habituation, the mouse was placed in the bright compartment, and after 300 s, the mouse gained access to the dark compartment. Upon entering the dark compartment, the door was closed, and a 0.3 mA electrical shock was delivered to the mouse's foot for 2 s as an adverse stimulus. Three hours after the training session, the animal was returned to the bright compartment and now had the option to avoid/enter the dark compartment. The latency period before the mouse entered the dark compartment was measured.

## 2.4. Statistical analysis

Where feasible, the experimenter was blinded to treatment to minimize any potential bias. Blinding was implemented for immunohistochemistry image acquisition and analysis and for behavioral testing and analysis. For electrophysiology experiments (MEA and patch-clamp) blinding was not possible because acute slice preparation and drug application required identification of treatment status. All data are expressed as mean ± or + standard error of mean (SEM). Outliers were identified and excluded using the Robust Regression and Outlier Removal (ROUT) method with a false discovery rate of 1%. The number of excluded points was recorded and reported in the results where applicable. The Shapiro-Wilk normality test was conducted to assess

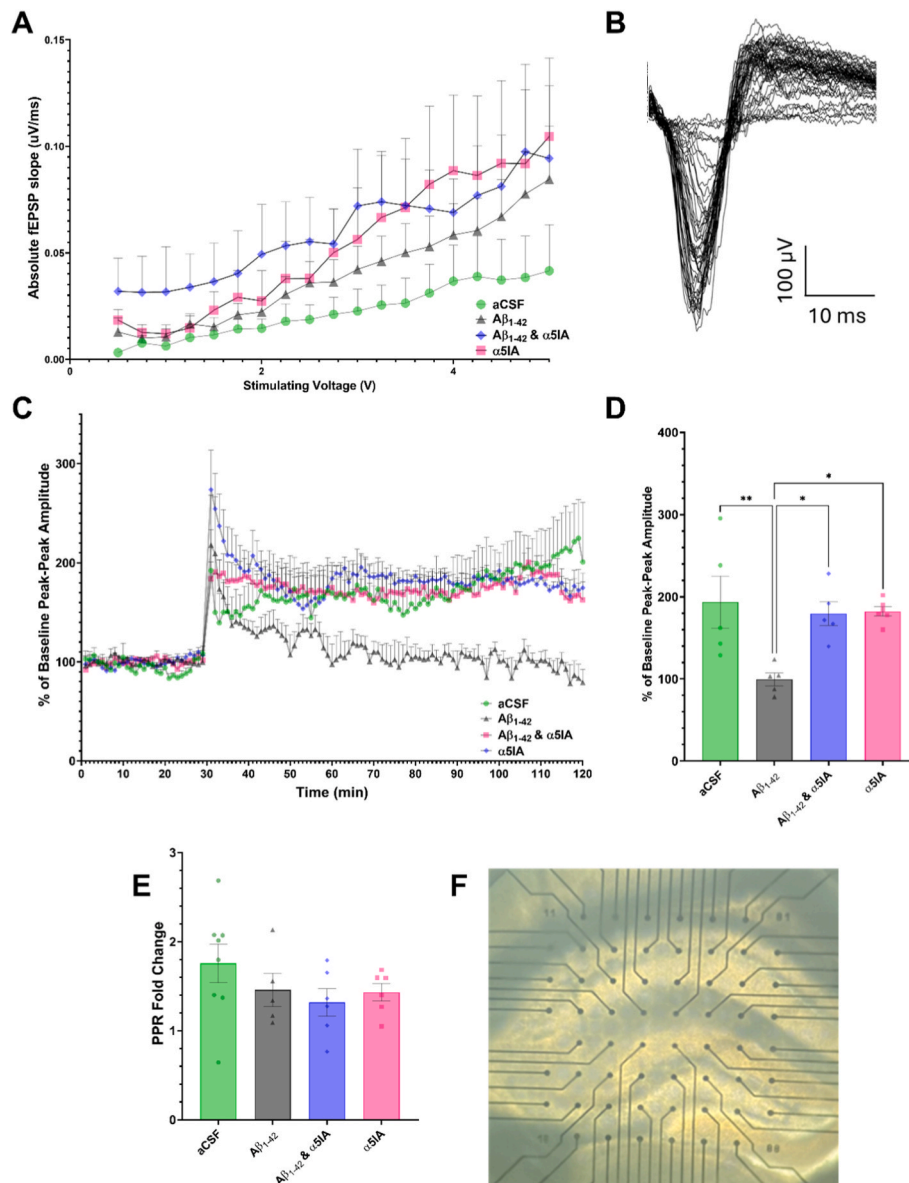


**Fig. 2. Effect of  $\alpha$ 5IA on A $\beta$ <sub>1-42</sub>-induced neuronal hyperexcitability and long-term potentiation impairments.** **A)** Input-output relationships in the stratum radiatum-CA1 network were measured for aCSF (n = 9), A $\beta$ <sub>1-42</sub> (n = 7), A $\beta$ <sub>1-42</sub> +  $\alpha$ 5IA (n = 10) or  $\alpha$ 5IA (n = 9) treated *ex vivo* hippocampal slices. Stimulating voltage from 0.5 to 5V were delivered and resulting fEPSP amplitude quantified **B)** Example traces of Input-output relationships in the pyramidal layer-CA1 network from an aCSF treated slice **C)** Timeline of normalized CA1 fEPSP amplitudes in the pyramidal layer-CA1 network for aCSF, A $\beta$ <sub>1-42</sub>, A $\beta$ <sub>1-42</sub> and  $\alpha$ 5IA or  $\alpha$ 5IA treated acute hippocampal brain slices. A $\beta$ <sub>1-42</sub>-treated slices exhibited markedly decreased potentiation post-theta-burst stimulation. **D)** Normalized fEPSP responses for 100-110 min (aCSF n = 5, A $\beta$ <sub>1-42</sub> n = 6, A $\beta$ <sub>1-42</sub> and  $\alpha$ 5IA n = 5 or  $\alpha$ 5IA n = 6 slices). **E)** Paired-pulse ratios in the pyramidal layer-CA1 network for aCSF (n = 8 slices), A $\beta$ <sub>1-42</sub> (n = 5 slices), A $\beta$ <sub>1-42</sub> and  $\alpha$ 5IA (n = 6 slices) or  $\alpha$ 5IA-treated (n = 7 slices) acute hippocampal brain slices. No significant differences in paired-pulse facilitation were observed. **F)** Acute hippocampal slices were positioned on a perforated microelectrode array. Data are expressed as mean ± SEM or + SEM (one-way ANOVA, Tukey's post-hoc test \*p < 0.01, \*\*p < 0.01, \*\*\*p < 0.001, \*\*\*\*p < 0.0001).

whether the data were normally distributed, and a Brown-Forsythe test was used to analyze the homogeneity of variance of the data. All data that passed these tests were analysed by one-way ANOVA followed by Tukey's post-hoc test. The YM and passive avoidance experiments did not pass normality or homogeneity of data variance tests and were analysed by a Kruskal-Wallis test, with Dunn's post hoc test used to examine differences between the different groups. The input-output experiments were assessed by repeated measures two-way ANOVA. All statistical analyses were conducted using Prism (version 10, GraphPad), and a P value equal to or < 0.05 was considered to indicate statistical significance.

### 3. Results

#### 3.1. Restoration of long-term potentiation by $\alpha 5IA$ in $\beta$ -amyloid 1-42 treated acute mouse hippocampal slices

To assess  $\alpha 5IA$ 's effect on  $A\beta_{1-42}$  - treated hippocampal slices, slices from male and female 4-8-month-old mice were incubated with aCSF,  $A\beta_{1-42}$ ,  $A\beta_{1-42}$  +  $\alpha 5IA$  or  $\alpha 5IA$  for 1 h prior to positioning on a MEA (Fig. 2F).  $A\beta_{1-42}$ 's effect on neuronal excitability was first assessed as measured by input-output curve analysis (Milior et al., 2016) (Fig. 2A and B). Input-output curves consist of a series of progressively increasing stimulation intensities and the corresponding evoked field potential responses. While indirect, the fold change in response amplitude to increasing inputs reflects the network's increasing responsiveness to an input. A co-treatment with  $A\beta_{1-42}$  and 1  $\mu M$   $\alpha 5IA$  (n = 10 slices) or either compound alone ( $A\beta_{1-42}$  n = 7 slices,  $\alpha 5IA$  n = 9 slices) showed a trend towards increased excitability versus aCSF treated slices (n = 9 slices), displaying increased absolute fEPSP slopes versus that of the control in the stratum radiatum (two-way repeated-measures, stimulating voltage and drug treatment showed no interaction ( $F(54,558) = 0.71$ ,  $p = 0.9438$ ). Stimulating voltage had a main effect ( $F(1.26, 38.93) = 16.6$ ,  $p < 0.0001$ ) but no effect of drug treatment ( $F(3,31) = 0.95$ ,  $p = 0.4268$ ), Fig. 2A and B).

LTP is a neuronal process critical for the formation of memories and commonly used for electrophysiological measurement of neuronal plasticity (O'Connell et al., 2024). A one-way ANOVA demonstrated a significant effect of treatment ( $F(3, 17) = 6.04$ ,  $p = 0.0054$ ). Following treatment with 100 nM  $A\beta_{1-42}$ , LTP was significantly reduced compared to control slices in the pyramidal layer ( $193.5 \pm 31.73$  vs  $99.43 \pm 7.795$ , aCSF (n = 5 slices) vs  $A\beta_{1-42}$  (n = 6 slices),  $p = 0.0077$ , Fig. 2C and D).

The treatment with 1  $\mu M$   $\alpha 5IA$  rescued this pathophysiology, restoring LTP to levels similar to the control ( $99.43 \pm 7.795$  vs  $179.7 \pm 14.73$ ,  $A\beta_{1-42}$  (n = 6 slices) vs  $A\beta_{1-42}$  &  $\alpha 5IA$  (n = 5 slices),  $p = 0.0243$ , Fig. 2C and D). Treatment with 100 nM  $\alpha 5IA$  demonstrated a trend indicative of LTP recovery (one-way ANOVA,  $F(3, 14) = 3.903$ ,  $p = 0.0322$ ;  $99.43 \pm 7.795$  vs  $143.4 \pm 31.04$ ,  $A\beta_{1-42}$  (n = 6 slices) vs  $A\beta_{1-42}$  & 100 nM  $\alpha 5IA$  (n = 3 slices),  $p = 0.5950$ , Figure S1 A & B).

Short-term plasticity was assessed by paired-pulse ratio, two data points were removed from the aCSF group, one from the  $A\beta_{1-42}$  group and one from the  $\alpha 5IA$  treatment group using the ROUT method prior to statistical analysis. There was no significant effect of treatment on paired-pulse ratio ( $F(3, 21) = 1.229$ ,  $p = 0.3241$ ),  $A\beta_{1-42}$  treatment did not affect short-term plasticity ( $1.758 \pm 0.217$  vs  $1.458 \pm 0.187$ , aCSF (n = 8 slices) vs  $A\beta_{1-42}$  (n = 5 slices),  $p = 0.660$ ). Similarly, no significant changes were seen following  $A\beta_{1-42}$  &  $\alpha 5IA$  treatment ( $1.758 \pm 0.217$  vs  $1.317 \pm 0.154$ , aCSF (n = 8 slices) vs  $A\beta_{1-42}$  &  $\alpha 5IA$  (n = 6 slices),  $p = 0.3050$ ) or treatment with  $\alpha 5IA$  alone ( $1.758 \pm 0.217$  vs  $1.432 \pm 0.098$ , aCSF (n = 8 slices) vs  $\alpha 5IA$  (n = 6 slices),  $p = 0.5571$ , Fig. 2E). Thus, *in vitro* acute  $\alpha 5IA$  treatment fully rescues  $A\beta_{1-42}$ -induced LTP impairments in the CA1 subregion of acute hippocampal slices.

#### 3.2. $\alpha 5IA$ -restores extrasynaptic GABA tonic inhibitory conductance in $\beta$ -amyloid 1-42-injected mice

Next,  $\alpha 5IA$ 's effect on  $A\beta_{1-42}$ -induced enhanced extrasynaptic GABA-mediated tonic conductance was assessed in 2-month-old mice. Seven days post  $A\beta_{1-42}$ -injection, mice were euthanized by cervical dislocation and acute brain slices were obtained. For  $\alpha 5IA$ -treated slices,  $\alpha 5IA$  was added to the patch-clamp recording aCSF solution, and a measurement of tonic conductance was obtained. One-way ANOVA revealed a significant effect of treatment ( $F(3, 12) = 11.23$ ,  $p = 0.0008$ ). As previously reported by our group (Calvo-Flores Guzman et al., 2020a), slices from  $A\beta_{1-42}$ -injected mice displayed significantly increased tonic conductance versus slices from naïve control ( $50.95 \pm 4.632$  vs  $78.07 \pm 8.923$ , Naive (n = 4 cells) vs  $A\beta_{1-42}$  (n = 5 cells),  $p = 0.0462$ ) and aCSF-injected mice ( $35.05 \pm 2.670$  vs  $78.07 \pm 8.923$ , aCSF (n = 4 cells) vs  $A\beta_{1-42}$  (n = 5 cells),  $p = 0.0022$ , Fig. 3A–E).  $\alpha 5IA$  treatment significantly decreased tonic inhibitory conductance versus slices from  $A\beta_{1-42}$ -injected mice, which did not have any treatment added to the recording chamber and were perfused with aCSF ( $78.07 \pm 8.923$  vs  $29.57 \pm 6.091$ ,  $A\beta_{1-42}$  s (n = 5 cells) vs  $A\beta_{1-42}$  &  $\alpha 5IA$  (n = 3 cells),  $p = 0.0016$ , Fig. 3A–E). At 100 nM,  $\alpha 5IA$  reduced the extrasynaptic tonic conductance in slices from  $A\beta_{1-42}$ -injected mice by  $64 \pm 6.09$  %, such that slices from  $A\beta_{1-42}$ -injected mice treated with  $\alpha 5IA$  were no longer significantly different from slices from naïve ( $50.95 \pm 4.632$  vs  $29.57 \pm 6.091$ , Naive (n = 4) vs  $A\beta_{1-42}$  &  $\alpha 5IA$  (n = 3),  $p = 0.2119$ ) or aCSF-injected mice ( $35.05 \pm 2.670$  vs  $29.57 \pm 6.091$ , aCSF (n = 4) vs  $A\beta_{1-42}$  &  $\alpha 5IA$  (n = 3),  $p = 0.9490$ ). Thus, *ex vivo* acute treatment with  $\alpha 5IA$  was able to reduce the enhanced extrasynaptic GABA-mediated tonic conductance seen in acute hippocampal slices from mice 7 days after intrahippocampal  $A\beta_{1-42}$  injection.

To determine the effects of  $\alpha 5IA$  on neuronal survival, 18-month-old  $A\beta_{1-42}$ -injected mice were treated with 1 mg/kg or 5 mg/kg  $\alpha 5IA$  twice daily, i.p for 30 days. These mice underwent behavioral testing, following which the tissue was processed for immunohistochemistry. One-way ANOVA revealed treatment had a significant effect on neuronal survival ( $F(6, 47) = 11.98$ ,  $p < 0.0001$ ).  $A\beta_{1-42}$ -injected mice had a significantly lower number of pyramidal cells versus naïve mice ( $34.38 \pm 1.012$  vs  $23.75 \pm 1.369$ , naïve mice (n = 8) vs  $A\beta$ -injected mice (n = 8),  $p < 0.0001$ , Fig. 3F and G), aCSF-injected mice ( $30.25 \pm 0.829$  vs  $23.75 \pm 1.369$ , aCSF-injected mice (n = 8) vs  $A\beta$ -injected mice (n = 8),  $p = 0.0094$ ) and scrambled  $A\beta$ -injected mice ( $29.50 \pm 0.945$  vs  $23.75 \pm 1.369$ , scrambled  $A\beta$ -injected mice (n = 7) vs  $A\beta$ -injected mice (n = 8),  $p = 0.0404$ ).

Unlike the findings from our laboratory (Vinnakota et al., 2020), where application of 100 nM of  $\alpha 5IA$  rescued cell loss in an *in vitro* AD mouse model, in the AD mouse model used in the present study, twice daily i.p administration of 1 mg/kg or 5 mg/kg  $\alpha 5IA$  during the 30 days following  $A\beta_{1-42}$  injection did not rescue pyramidal cell loss in the CA1 region of the hippocampus ( $25.00 \pm 1.044$  vs  $23.75 \pm 1.369$ ,  $A\beta_{1-42}$  &  $\alpha 5IA$  1 mg (n = 8) vs  $A\beta$ -injected mice (n = 8),  $p = 0.9912$ ;  $23.57 \pm 1.856$  vs  $23.75 \pm 1.369$ ,  $A\beta_{1-42}$  &  $\alpha 5IA$  5 mg (n = 7) vs  $A\beta$ -injected mice (n = 8),  $p > 0.9999$ , Fig. 3F and G).

#### 3.3. Effect of $\alpha 5IA$ treatment on the cognitive performance of $\beta$ -amyloid 1-42-injected mice

To determine the effect of the  $\alpha 5IA$  treatment on  $A\beta_{1-42}$ -induced chronic long-term spatial memory impairment, 18-month-old mice were injected with  $A\beta_{1-42}$  following which two different doses of  $\alpha 5IA$  were administered twice a day for 30 days. Cognitive performance was measured using a battery of behavioral tests including the NOAL, NOR, MWM and YM and passive avoidance tests. The OM was used as a measure of anxiety. All behavioural tests were performed between day 7 and day 30 post  $A\beta_{1-42}$  injection (Fig. 1).

Administration of 1 and 5 mg/kg  $\alpha 5IA$  was found to rescue long-term spatial memory impairment in  $A\beta_{1-42}$ -injected mice, as indicated by the

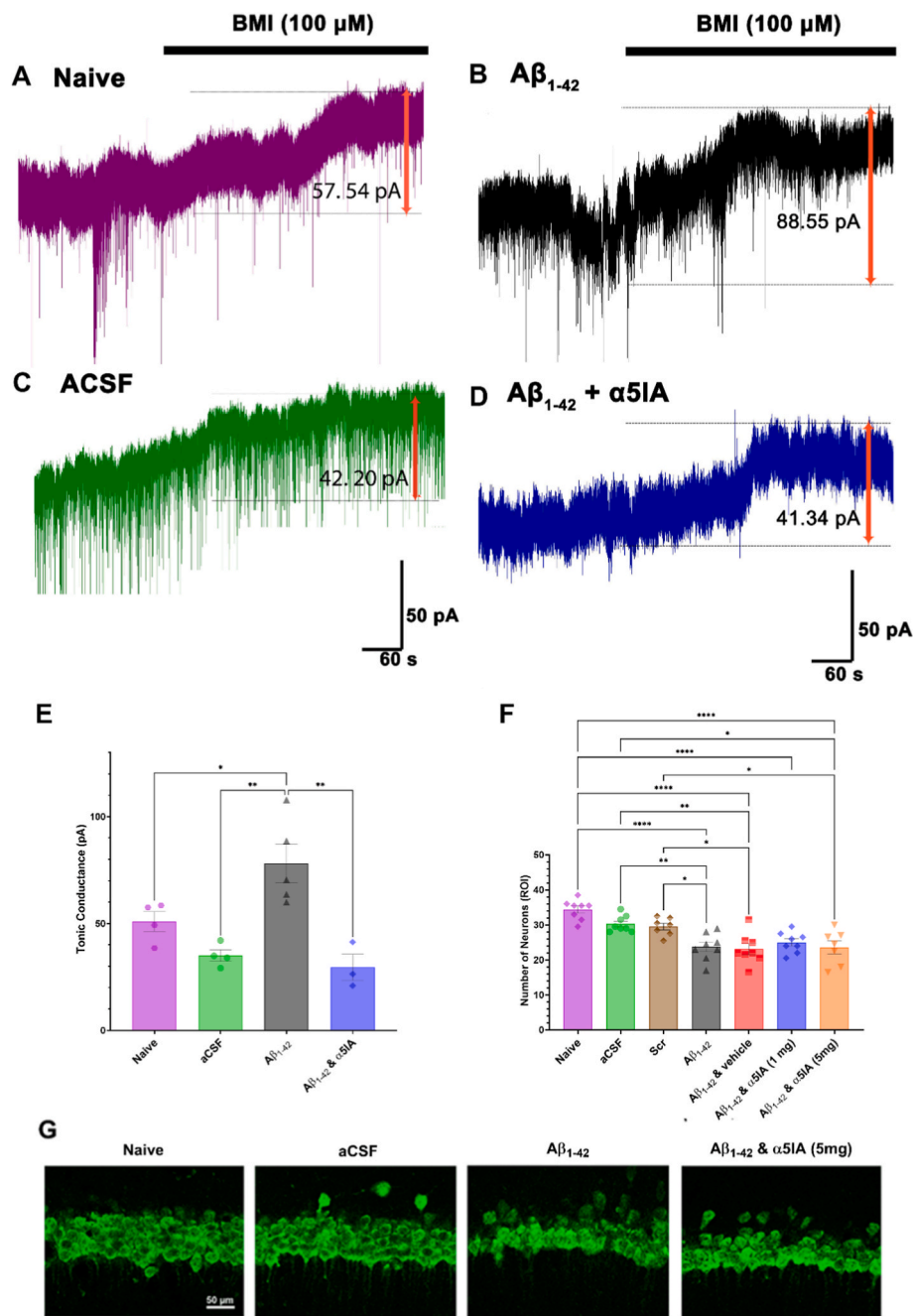


**Fig. 3.** Effect of  $\alpha 5IA$  on  $A\beta_{1-42}$ -induced increased tonic inhibitory conductance and pyramidal cell loss in the CA1 region of the hippocampus. **A-D)** Representative whole-cell voltage-clamp recording traces showing tonic inhibitory conductance induced by the addition of bicuculline methiodate (BMI) (100 nM) in acute hippocampal slices from **A)** naïve mice, **B)**  $A\beta_{1-42}$ -injected mice, **C)** ACSF-injected mice and in **D)**  $A\beta_{1-42}$ -injected mice treated with  $\alpha 5IA$  (100 nM) *ex vivo*. **E)** The average tonic inhibitory conductance in slices from  $A\beta_{1-42}$ -injected mice ( $n = 5$ ),  $A\beta_{1-42}$ -injected mice treated with 100 nM  $\alpha 5IA$  *ex vivo* ( $n = 3$ ), naïve control mice ( $n = 4$ ) and ACSF-injected mice ( $n = 4$ ).  $\alpha 5IA$  induced a significant decrease in tonic conductance in the  $A\beta_{1-42}$ -injected mice. **F)** The number of NeuN-positive pyramidal cells from the stratum pyramidale of the CA1 region of the hippocampus in naïve ( $n = 8$ ), ACSF-injected ( $n = 8$ ), scrambled  $A\beta$  (Scr)-injected ( $n = 7$ ), and  $A\beta_{1-42}$ -injected mice ( $n = 8$ ), and  $A\beta_{1-42}$ -injected mice treated with vehicle, 1 mg/kg  $\alpha 5IA$  or 5 mg/kg  $\alpha 5IA$  ( $n = 8$  and  $7$  respectively), at 30 days after  $A\beta_{1-42}$  injection. **G)** Representative images of NeuN-positive pyramidal cell counts. Data are expressed as mean  $\pm$  SEM (One-way ANOVA, Tukey's post-hoc test, \* $p < 0.05$ , \*\* $p < 0.01$ , \*\*\* $p < 0.001$ , \*\*\*\* $p < 0.0001$ ).

findings of the NOAL, NOR and MWM tests (Fig. 4A, B, C, respectively).  $A\beta_{1-42}$ -injected mice treated with 1 mg/kg and 5 mg/kg  $\alpha 5IA$  exhibited significantly better cognitive performance than the non-treated  $A\beta_{1-42}$ -injected mice in the NOAL test (one-way ANOVA,  $F(6, 76) = 8.493$ ,  $p < 0.0001$ ; with Tukey's post-hoc  $-0.190 \pm 0.069$  vs  $0.160 \pm 0.057$ ,  $A\beta_{1-42}$  vs  $A\beta_{1-42}$  &  $\alpha 5IA$  (1 mg),  $p = 0.0001$ ;  $-0.190 \pm 0.069$  vs  $0.191 \pm 0.048$ ,  $A\beta_{1-42}$  vs  $A\beta_{1-42}$  &  $\alpha 5IA$  (5 mg),  $p < 0.0001$ , Fig. 4A), and similar discrimination ratios were obtained for mice treated with both

doses of  $\alpha 5IA$ .

Likewise, the NOR results indicated that both doses of  $\alpha 5IA$  rescued long-term spatial memory impairment in  $A\beta_{1-42}$ -injected mice. That is,  $A\beta_{1-42}$ -injected mice treated with 1 mg/kg or 5 mg/kg of  $\alpha 5IA$  exhibited better cognitive performance than the non-treated  $A\beta_{1-42}$ -injected mice (One-way ANOVA ( $F(6, 71) = 9.469$ ,  $p < 0.0001$ ); with Tukey's post-hoc  $-0.055 \pm 0.078$  vs  $0.373 \pm 0.092$ ,  $A\beta_{1-42}$  vs  $A\beta_{1-42}$  &  $\alpha 5IA$  (1 mg),  $p = 0.0032$ ;  $-0.055 \pm 0.078$  vs  $0.421 \pm 0.102$ ,  $A\beta_{1-42}$  vs  $A\beta_{1-42}$  &  $\alpha 5IA$

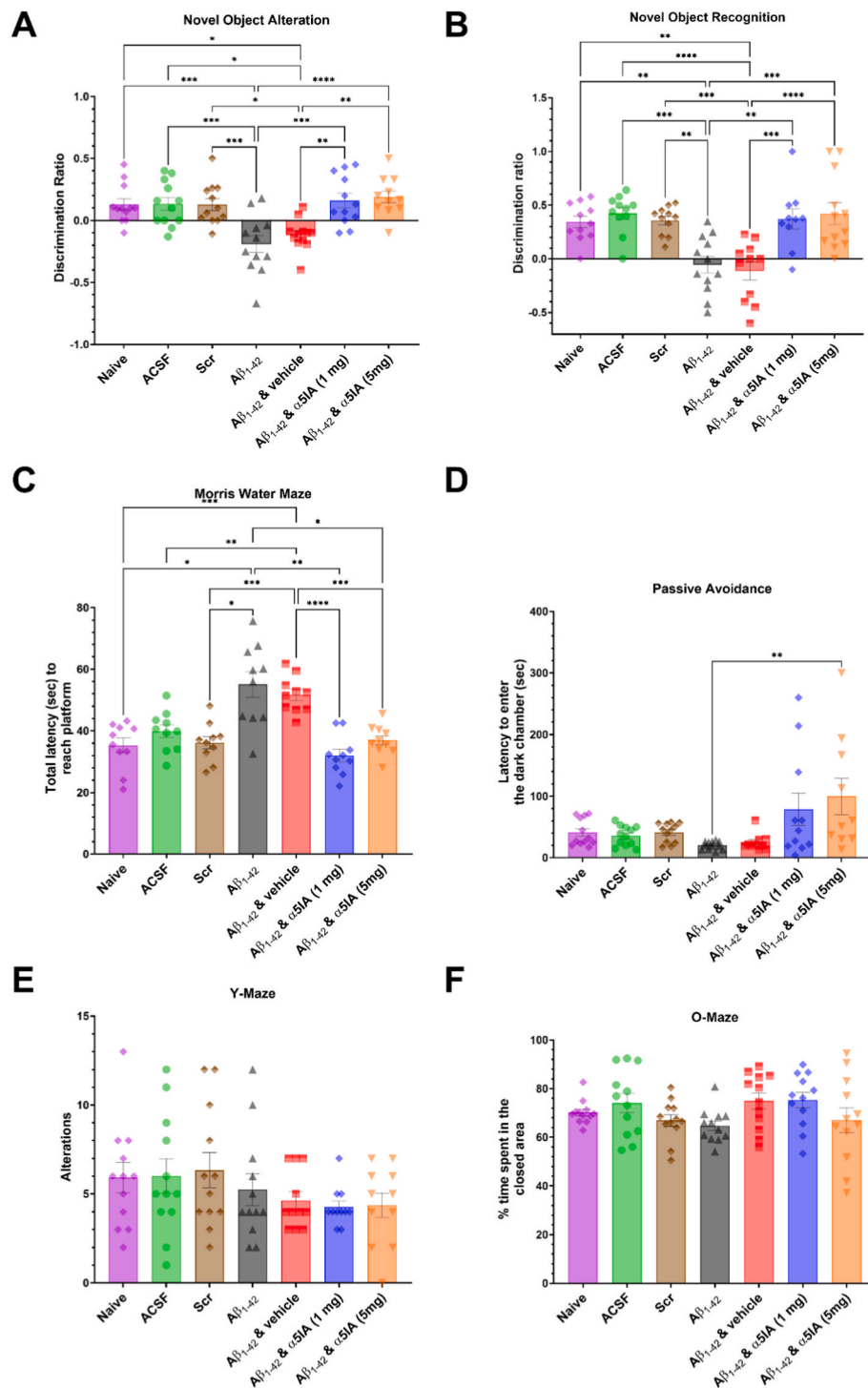


**Fig. 4.** Effect of  $\alpha 5IA$  treatment on  $A\beta_{1-42}$ -induced cognitive impairment. **A)** Novel object alteration test (performed on day 7 and 8) shows the discrimination ratio for novel object over a familiar object for naïve, ACSF-injected, scrambled  $A\beta$  (Scr)-injected,  $A\beta_{1-42}$ -injected,  $A\beta_{1-42}$ -injected mice treated with vehicle,  $A\beta_{1-42}$ -injected mice treated with 1 mg/kg of  $\alpha 5IA$  and  $A\beta_{1-42}$ -injected mice treated with 5 mg/kg of  $\alpha 5IA$  **B)** Novel object recognition test (performed on day 11 and 12) shows the discrimination ratio for the same treatment groups. **C)** Morris water maze (performed on day 20-24) shows the total latency in seconds to reach the platform for the same treatment groups. **D)** The passive avoidance test (performed on day 27) describes the latency to enter the dark chamber for all the groups mentioned above. **E)** Y-maze test (performed on day 15) shows the alternation percentage, which was calculated as the percentage of the ratio of actual to possible alternations. **F)** The O-maze (performed on day 17) shows the percentage of time spent in the closed area, which was considered as the amount of time spent in avoiding the new environment. Data are expressed as mean  $\pm$  SEM (A-C, F; one-way ANOVA, Tukey's post-hoc test; D & E as determined by Kruskal-Wallis and Dunn's multiple comparison test) (\* $P < 0.05$ , \*\* $P < 0.01$ , \*\*\* $P < 0.001$ , \*\*\*\* $P < 0.0001$ ,  $n = 10-12$  animals).

(5 mg),  $p = 0.0031$ ) and the vehicle-treated  $A\beta_{1-42}$ -injected mice ( $-0.114 \pm 0.085$  vs  $0.373 \pm 0.092$ ,  $A\beta_{1-42}$  & vehicle vs  $A\beta_{1-42}$  &  $\alpha 5IA$  (1 mg),  $p = 0.0007$ ;  $-0.114 \pm 0.085$  vs  $0.421 \pm 0.102$ ,  $A\beta_{1-42}$  & vehicle vs  $A\beta_{1-42}$  &  $\alpha 5IA$  (5 mg),  $p < 0.0001$  (Fig. 4B).

In the MWM test, treatment had a significant effect on the total latency period to reach the platform (average value for day 1 to day 4, one-way ANOVA,  $F(6, 63) = 13.06$ ,  $p < 0.0001$ ).  $\alpha 5IA$ -treated mice (1 and 5 mg/kg) required significantly less time to reach the platform than the non-treated  $A\beta_{1-42}$ -injected mice ( $55.07 \pm 4.196$  vs  $32.04 \pm 2.056$ ,  $A\beta_{1-42}$  vs  $A\beta_{1-42}$  &  $\alpha 5IA$  (1 mg),  $< 0.0001$ ;  $55.07 \pm 4.196$  vs  $36.99 \pm 1.512$ ,  $A\beta_{1-42}$  vs  $A\beta_{1-42}$  &  $\alpha 5IA$  (5 mg),  $< 0.0001$ ) and the vehicle-treated  $A\beta_{1-42}$ -injected mice ( $51.73 \pm 1.871$  vs  $32.04 \pm 2.056$ ,  $A\beta_{1-42}$  & vehicle vs  $A\beta_{1-42}$  &  $\alpha 5IA$  (1 mg),  $p < 0.0001$ ;  $51.73 \pm 1.871$  vs  $36.99 \pm 1.512$ ,  $A\beta_{1-42}$  & vehicle vs  $A\beta_{1-42}$  &  $\alpha 5IA$  (5 mg),  $0.0013$ , Fig. 4C & S3 A-I).

According to the passive avoidance test results, there was no significant difference in cognitive performance between the  $A\beta_{1-42}$ -injected mice treated with 1 mg/kg of  $\alpha 5IA$  and the non-treated or vehicle-treated  $A\beta_{1-42}$ -injected mice ( $78.82 \pm 26.22$  vs  $19.92 \pm 1.889$ ,  $A\beta_{1-42}$  &  $\alpha 5IA$  (1 mg) vs  $A\beta_{1-42}$ ,  $p = 0.2082$ ;  $78.82 \pm 26.22$  vs  $24.90 \pm 4.368$ ,  $A\beta_{1-42}$  &  $\alpha 5IA$  (1 mg) vs  $A\beta_{1-42}$  & vehicle,  $p > 0.9999$ ). However, treatment did have a significant effect on the latency to enter the dark chamber (Kruskal-Wallis test,  $H(6) = 18.95$ ,  $p = 0.0043$ ). Mice treated with 5 mg/kg of  $\alpha 5IA$  took a significantly longer time than the  $A\beta_{1-42}$ -injected mice to enter the dark chamber after the shock stimulus ( $99.80 \pm 29.52$  vs  $19.92 \pm 1.889$ ,  $A\beta_{1-42}$  &  $\alpha 5IA$  (5 mg) vs  $A\beta_{1-42}$ ,  $p = 0.0059$ , Fig. 4D). This suggests that the lower  $\alpha 5IA$  dose has no effect on non-spatial memory, and  $A\beta_{1-42}$ -injected mice do not show non-spatial memory deficits in line with our earlier findings; however, treatment with the higher  $\alpha 5IA$  dose (5 mg/kg) improved non-spatial memory in  $A\beta_{1-42}$ -injected mice (Calvo-Flores Guzman et al., 2020b).

According to the findings of the YM test, treatment had no effect on short-term memory (Kruskal-Wallis test,  $H(6) = 4.69$ ,  $p = 0.5848$ ).  $A\beta_{1-42}$ -injection had no significant effect on short-term memory ( $5.250 \pm 0.889$  vs  $5.917 \pm 0.857$ ,  $A\beta_{1-42}$  vs naïve,  $p > 0.9999$ ). Mice treated with  $\alpha 5IA$  (1 and 5 mg/kg) did not show any significant difference regarding the number of alternations (percentage of correct alternations) compared with  $A\beta_{1-42}$ -injected and vehicle-treated  $A\beta_{1-42}$ -injected mice ( $5.250 \pm 0.889$  vs  $4.636 \pm 0.491$  vs  $4.273 \pm 0.333$  vs  $4.364 \pm 0.678$ ,  $A\beta_{1-42}$  vs  $A\beta_{1-42}$  & vehicle vs  $A\beta_{1-42}$  &  $\alpha 5IA$  (1 mg) vs  $A\beta_{1-42}$  &  $\alpha 5IA$  (5 mg),  $p > 0.9999$ , Fig. 4E). Thus,  $\alpha 5IA$  treatment does not affect short-term spatial memory in  $A\beta_{1-42}$ -injected mice.

No significant difference was found in anxiety levels, as assessed by the OM test (One-way ANOVA,  $F(6, 77) = 1.767$ ,  $p = 0.1171$ ). Tukey's post-hoc analysis revealed no significant difference between the non-injected or vehicle-injected and the  $A\beta_{1-42}$ -injected mice ( $5.917 \pm 0.857$  vs  $6.000 \pm 0.977$  vs  $6.333 \pm 0.987$  vs  $5.250 \pm 0.889$ , Naïve vs ACSF vs Scr vs  $A\beta_{1-42}$ ,  $p > 0.9999$ ). Additionally,  $A\beta_{1-42}$ -injected mice treated with either dose of  $\alpha 5IA$  did not spend a significantly different amount of time in the closed arms in the OM test ( $5.250 \pm 0.889$  vs  $4.273 \pm 0.333$  vs  $4.364 \pm 0.678$ ,  $A\beta_{1-42}$  vs  $A\beta_{1-42}$  &  $\alpha 5IA$  (1 mg) vs  $A\beta_{1-42}$  &  $\alpha 5IA$  (5 mg),  $p > 0.9999$ ); thus,  $A\beta_{1-42}$  injection and  $\alpha 5IA$  treatment had no anxiogenic effect (Fig. 4F). All the tested groups spent a similar amount of time in the closed arms of the O-maze apparatus. The total distance travelled and the speed of the animal movement in the arena during the NOAL and NOR habituation period were used as measures of exploration and motor function. No significant differences were found in the travelled distance (or speed) between the different experimental groups, indicating no differences in anxiety levels and a normal motor function (Figure S2 A-D).

#### 4. Discussion

It has been well established that the E/I balance is disrupted in the AD brain, an occurrence that has been proposed to underlie the cognitive deficits characteristic of the disease (Francis, 2005; Vinnakota et al., 2020; Govindpani et al., 2017; Ratner et al., 2021). As therapies

targeting the excitatory neurotransmitter systems currently do not prevent disease progression, targeting inhibitory neurotransmission to restore the E/I imbalance represents a promising alternative therapeutic strategy for the treatment of AD. To assess the therapeutic potential of targeting the GABAergic system, we performed electrophysiological and behavioral tests using  $\alpha 5IA$ , an  $\alpha 5$ -GABAAR inverse agonist with *ex vivo* and *in vivo* AD models. The subsequent analysis revealed that  $\alpha 5IA$  reduced  $A\beta$ -induced learning and memory deficits in NOAL, NOR, and MWM tests, ameliorated the  $A\beta$ -induced increase in tonic conductance and improved  $A\beta$ -induced LTP deficits.

*Ex vivo* microelectrode array analysis showed that within the CA1 subregion stratum radiatum,  $A\beta_{1-42}$  application showed a trend towards increased neuronal excitability, evidenced by an elevation in fEPSP slope in response to input stimulation. This finding aligns with previous preclinical studies reporting an initial hyperexcitable state induced by acute application of  $A\beta_{1-42}$  (Tamagnini et al., 2015; Varga et al., 2014; Sánchez-Rodríguez et al., 2017, 2019; Wang et al., 2020). Notably, acute *ex vivo* co-treatment or treatment with  $\alpha 5IA$  alone also shows a trend towards increased excitability, likely due to  $\alpha 5IA$ 's mechanism of action as a selective negative allosteric modulator of  $\alpha 5$ -GABAARs. These receptors contribute to tonic inhibitory conductance (Lee and Maguire, 2014), thus their inhibition would reduce this tonic or baseline inhibition, ultimately resulting in an increased excitatory drive within the neuronal network (Song et al., 2011). LTP, a prolonged enhancement of excitatory synaptic transmission, serves as a key measure of memory and learning in *ex vivo* AD research (Liu et al., 2020; Choi et al., 2023). Consistent with earlier studies,  $A\beta_{1-42}$  treatment significantly decreased LTP (O'Connell et al., 2024); however, acute  $\alpha 5IA$  treatment ameliorated these  $A\beta$ -induced LTP deficits. Previous *ex vivo* studies have demonstrated that  $\alpha 5IA$  potentiates LTP in wild-type animals, although the underlying mechanism is unclear (Dawson et al., 2006; Atack, 2008). Our research has previously shown that  $A\beta_{1-42}$ -injected mice exhibited significant increases in extrasynaptic tonic conductance in the stratum pyramidale of the CA1 hippocampal region and impaired long-term spatial memory (Calvo-Flores Guzman et al., 2020a). Increased extrasynaptic tonic conductance has also been observed in the dentate gyrus (DG) of a 5xFAD AD mouse model, which was associated with cognitive decline (Wu et al., 2014b). Based on these findings we hypothesized that the improvement in LTP was linked to the restoration of physiological tonic GABA inhibitory conductance. While  $\alpha 5IA$ 's ability to reduce tonic conductance has previously been shown in primary mouse hippocampal neurons (Manzo et al., 2021), this study was among the first to evaluate  $\alpha 5IA$ 's ability to reduce tonic conductance in an AD model. Patch clamp slice experiments demonstrated that tonic conductance in  $A\beta_{1-42}$ -injected mouse hippocampal slices acutely treated with  $\alpha 5IA$  *ex vivo* was no longer significantly different from naïve or ACSF-injected mice. With regard to the effect of *in vivo*  $\alpha 5IA$  drug treatment on  $A\beta_{1-42}$ -induced cell loss, there was a lack of cell rescue following  $\alpha 5IA$  treatment. This contrasts *in vitro* results previously reported by our laboratory (Vinnakota et al., 2020). However, *in vitro*, administration of  $\alpha 5IA$  and  $A\beta_{1-42}$  occurred simultaneously, leading to an immediate effect on cell survival. In contrast, when the drug is administered *in vivo*, a longer period is required before the drug effectively reaches the injection site, and the neurons might have suffered extensive irreversible damage by this time. Another factor which may contribute to this discrepancy is the variability of  $\alpha 5IA$  exposure *in vivo* due to its short half-life, in comparison to the constant levels achieved in culture (Atack, 2010). Our results demonstrated that  $A\beta_{1-42}$ -injected mice showed hippocampal-dependent long-term spatial memory impairment, as indicated by the results of the NOAL, NOR and MWM tests. Although pharmacological inhibition of  $\alpha 5$ -GABAARs by  $\alpha 5IA$  did not reverse neuronal loss, it improved hippocampal-dependent long-term spatial memory in  $A\beta_{1-42}$ -injected mice. Given the short interval between  $\alpha 5IA$  treatment and behavioral testing, the observed effect may reflect both acute pharmacological actions as well as ongoing modulatory effects of chronic  $\alpha 5IA$  dosing.

The data presented here suggest that in both *ex vivo* and *in vivo* AD models,  $\alpha 5$ IA improves cognitive function by restoring CA1 tonic inhibition, thereby re-establishing E/I balance and ameliorating the abnormal hippocampal network activity induced by  $A\beta_{1-42}$ . Prior studies using  $\alpha 5$ -deficient mice support this hypothesis, as the enhanced performance in learning tasks was mediated by decreased GABAergic synaptic inhibition in the hippocampus, as measured by evoked and spontaneous inhibitory post-synaptic potentials recorded from CA1 pyramidal neurons (Collinson et al., 2002). However, the precise mechanism by which reduced tonic inhibition enhances hippocampal network function and cognitive performance remains to be elucidated. Given that tonic inhibition is a key regulator of hippocampal pyramidal cell excitability,  $\alpha 5$ IA's restoration of physiological tonic inhibition may restore pyramidal neuron excitability and thus improve network function. Additionally, PV-positive inhibitory interneurons in the CA1 not only target pyramidal cells but also form synaptic connections with other inhibitory neurons (Bezaire and Soltesz, 2013; Gulyás et al., 1999). Thus, the abnormal hippocampal network activity characteristic of AD may result from a combination of two opposing mechanisms; altered pyramidal cell excitability and disinhibition of inhibitory interneuron networks leading to overactivation of pyramidal cells (Kammel et al., 2018).  $\alpha 5$ IA may counteract both effects, normalizing network activity, enhancing LTP and supporting cognitive function. Supporting this, recent work revealed that  $\alpha 5$ -GABAARs can redistribute to inhibitory synapses in an activity-dependent manner, where they suppress NMDAR-dependent induction for further LTP (Davenport et al., 2021). This provides a potential mechanistic link for  $\alpha 5$ IA modulation of  $\alpha 5$ -GABAARs to restore hippocampal network function.

Another important factor to consider is the role of tonic inhibition in mediating network oscillations in the hippocampus. Fast-spiking PV-positive interneurons mediate hippocampal network oscillations, which are crucial for learning and memory processes (Bartos et al., 2007; Mann and Paulsen, 2007; Giovannetti et al., 2018) used an optogenetic approach to demonstrate that the restoration of theta oscillations in an APP/PS1 AD mouse model ameliorated cognitive decline. (Iaccarino et al., 2016) reported that reduced gamma oscillations preceded cognitive impairment in a mouse model of AD, with the cognitive symptoms being reversed by the optogenetic activation of fast-spiking PV + interneurons. Importantly, aberrant gamma oscillations have been found in many AD mouse models (Palop et al., 2007; Verret et al., 2012; Gillespie et al., 2016), and abnormalities in oscillatory activity and dysfunctional network synchrony have been confirmed in AD patients (Mucke, 2018). Evidence shows a direct link between  $\alpha 5$ -GABAARs and gamma oscillations (20–80 Hz); *ex vivo* hippocampal slices from  $\alpha 5^{-/-}$  mice reportedly display increased kainate-induced gamma oscillations (Towers et al., 2004). These gamma oscillations participate in the coordination of neuronal network activity, particularly cognitive processes (Mann et al., 2005). Therefore, another plausible explanation for  $\alpha 5$ -mediated enhancements in cognition may be the restoration of gamma oscillations and hippocampal rhythms. Based on the extensive data on  $A\beta_{1-42}$ -induced cognitive decline in AD, dysfunctional hippocampal network activity and the mediation of oscillatory activity by enhanced tonic inhibition in the hippocampus, the pro-cognitive effects mediated by  $\alpha 5$ IA are likely a consequence of (1) its action on hippocampal PV + interneurons through the restoration of gamma oscillations and synchronization of hippocampal network circuitry, and (2) its effect on principal hippocampal pyramidal neurons by restoring excitatory synaptic transmission, mechanisms which should be comprehensively explored in future studies.

In the present study, our observations of cognitive restoration mediated by  $\alpha 5$ IA provide an insight into the contribution of  $A\beta_{1-42}$  to cognitive decline seen in AD, raising the possibility of a promising therapeutic approach. These findings confirm the pharmacological potential of  $\alpha 5$ IA in restoring AD cognitive-like symptoms in the rodent brain. However, a limitation of the present study is the use of animals of different ages across experimental techniques, with electrophysiological

techniques (patch-clamp and MEA studies), requiring the use of younger animals, which may introduce age-dependent effects and limit direct comparability across experiments. Although  $\alpha 5$ IA displays promising results in the AD models explored here, prolonged use, as would be required for AD treatment, has been reported to cause high-dose renal toxicity (Atack, 2010). Consequently, future research may focus on alternative  $\alpha 5$  NAMs, such as ONO-8590580, which has shown pre-clinical efficacy (Kawaharada et al., 2018) and basmisanil, which has shown a favorable safety profile in clinical trials (Goeldner et al., 2022), although their potential in AD has not yet been explored. The data presented here highlight that targeting  $\alpha 5$ -GABAARs with inverse agonists may be a promising and important direction for the development of novel therapies for the treatment of AD, and for further drug development to identify the ideal  $\alpha 5$ -GABAAR targeting drug.

### CRediT authorship contribution statement

**Aoife O'Connell:** Writing – review & editing, Writing – original draft, Visualization, Project administration, Methodology, Investigation, Funding acquisition, Formal analysis, Data curation. **Beatriz Calvo-Flores Guzmán:** Writing – review & editing, Writing – original draft, Visualization, Methodology, Investigation, Funding acquisition, Formal analysis, Data curation, Conceptualization. **Ying Zhai:** Writing – review & editing, Writing – original draft, Visualization, Methodology, Investigation, Formal analysis, Data curation. **Cameron N. Keighron:** Writing – review & editing, Methodology, Investigation, Formal analysis. **Jordi Boix:** Writing – review & editing, Writing – original draft, Investigation, Formal analysis, Data curation. **Katie Peppercorn:** Writing – review & editing, Writing – original draft, Methodology, Investigation. **Warren P. Tate:** Writing – review & editing, Writing – original draft, Validation, Supervision, Resources, Methodology, Investigation, Funding acquisition. **Henry J. Waldvogel:** Writing – review & editing, Writing – original draft, Supervision, Resources, Investigation, Formal analysis. **Richard LM. Faull:** Writing – review & editing, Writing – original draft, Supervision, Resources, Investigation, Funding acquisition, Formal analysis. **Johanna M. Montgomery:** Writing – review & editing, Writing – original draft, Supervision, Resources, Methodology, Investigation, Funding acquisition, Formal analysis, Data curation. **Leo Quinlan:** Writing – review & editing, Writing – original draft, Supervision, Resources, Methodology, Formal analysis. **Andrea Kwakowsky:** Writing – review & editing, Writing – original draft, Visualization, Validation, Supervision, Resources, Project administration, Methodology, Investigation, Funding acquisition, Formal analysis, Data curation, Conceptualization.

### Ethics approval and consent to participate

All experiments were approved and performed within the regulations of the University of Galway Animal Care and Research Ethics Committee (approval number: 2022.10.002) and the University of Auckland Animal Ethics Committee (approval numbers: 001586 and 001655).

### Consent for publication

Not applicable.

### Funding

This work was supported by the University of Galway Hardiman Research Scholarship (A.O. and A.K.); Alzheimers New Zealand (A.K.; 3718869); Freemasons New Zealand (A.K.; 3719321); Alzheimers New Zealand Charitable Trust (A.K.; 502575); Aotearoa Foundation, New Zealand (A.K.; 3705579); Brain Research New Zealand (B.C.F.G., J.M., H.J.W., R.L.F., A.K.; 3710638); Health Research Council of New Zealand (R.L.F., H.J.W., A.K.; 3723033), Otago Medical School and the

Department of Physiology, University of Otago (A.K.; 110089.01).

## Declaration of competing interest

None.

## Acknowledgements

We thank Dr Daniel Kerr, Dr Claire Feerick, Barbara Coen, and Kristina Hubbard for excellent work and assistance, members of the Montgomery and Quinlan labs for practical and theoretical electrophysiological assistance, and members of the Vernon Jansen Unit, University of Auckland and the Bio-Resources Unit, University of Galway for excellent work.

## Appendix A. Supplementary data

Supplementary data to this article can be found online at <https://doi.org/10.1016/j.neuropharm.2026.110892>.

## Data availability

All datasets generated and analysed supporting the findings of this study are available on request from the corresponding author and will be made openly available upon publication.

## References

- Abrahamsson, T., Lalanne, T., Watt, A.J., Sjöström, P.J., 2016. Long-term potentiation by theta-burst stimulation using extracellular field potential recordings in acute hippocampal slices. *Cold Spring Harb. Protoc.* 2016. <https://doi.org/10.1101/pdb.prot091298> <https://doi.org/10.1101/pdb.prot091298>.
- Alia, A., Roßner, S., 2018. Gender, GABAergic dysfunction and AD. *Aging (Albany NY)* 10, 3636–3637. <https://doi.org/10.18632/aging.101672>.
- 2023 Alzheimer's disease facts and figures. *Alzheimer's Dement.* 19, 2023, 1598–1695. <https://doi.org/10.1002/alz.13016>.
- Arandjelović, J., et al., 2022. Effects of  $\alpha 5$  GABA(A) receptor modulation on social interaction, memory, and neuroinflammation in a mouse model of Alzheimer's disease. *CNS Neurosci. Ther.* 28, 1767–1778. <https://doi.org/10.1111/cns.13914>.
- Atack, J.R., 2008. GABA(A) receptor subtype-selective efficacy: TPA023, an alpha2/alpha3 selective non-sedating anxiolytic and alpha5A, an alpha5 selective cognition enhancer. *CNS Neurosci. Ther.* 14, 25–35. <https://doi.org/10.1111/j.1527-3458.2007.00034.x>.
- Atack, J.R., 2010. Preclinical and clinical pharmacology of the GABA(A) receptor alpha5 subtype-selective inverse agonist alpha5A. *Pharmacol. Ther.* 125, 11–26. <https://doi.org/10.1016/j.pharmthera.2009.09.001>.
- Atack, J.R., et al., 2009a. The plasma-occupancy relationship of the novel GABA(A) receptor benzodiazepine site ligand, alpha5A, is similar in rats and primates. *Br. J. Pharmacol.* 157, 796–803. <https://doi.org/10.1111/j.1476-5381.2009.00216.x>.
- Atack, J.R., et al., 2009b. In vitro and in vivo properties of 3-tert-butyl-7-(5-methylisoxazol-3-yl)-2-(1-methyl-1H-1,2,4-triazol-5-ylmethoxy)-pyrazolo[1,5-d][1,2,4]triazine (MRK-016), a GABA(A) receptor alpha5 subtype-selective inverse agonist. *J. Pharmacol. Exp. Therapeut.* 331, 470–484. <https://doi.org/10.1124/jpet.109.157636>.
- Bartos, M., Vida, I., Jonas, P., 2007. Synaptic mechanisms of synchronized gamma oscillations in inhibitory interneuron networks. *Nat. Rev. Neurosci.* 8, 45–56. <https://doi.org/10.1038/nrn2044>.
- Bernardo, A.M., et al., 2025. Pro-cognitive and neurotrophic benefits of  $\alpha 5$ -GABA-A receptor positive allosteric modulation in a  $\beta$ -amyloid deposition mouse model of Alzheimer's disease pathology. *Neurobiol. Aging* 147, 49–59. <https://doi.org/10.1016/j.neurobiolaging.2024.12.001>.
- Bezaire, M.J., Soltesz, I., 2013. Quantitative assessment of CA1 local circuits: knowledge base for interneuron-pyramidal cell connectivity. *Hippocampus* 23, 751–785. <https://doi.org/10.1002/hipo.22141>.
- Bi, D., Wen, L., Wu, Z., Shen, Y., 2020. GABAergic dysfunction in excitatory and inhibitory (E/I) imbalance drives the pathogenesis of Alzheimer's disease. *Alzheimer's Dement.* 16, 1312–1329. <https://doi.org/10.1002/alz.12088>.
- Braudeau, J., et al., 2011a. Specific targeting of the GABA-A receptor  $\alpha 5$  subtype by a selective inverse agonist restores cognitive deficits in Down syndrome mice. *J. Psychopharmacol.* 25, 1030–1042. <https://doi.org/10.1177/0269881111405366>.
- Braudeau, J., et al., 2011b. Chronic treatment with a promnesiant GABA-A  $\alpha 5$ -selective inverse agonist increases immediate early genes expression during memory processing in mice and rectifies their expression levels in a Down Syndrome mouse model. *Adv. Pharmacol. Sci.* 2011, 153218. <https://doi.org/10.1155/2011/153218>.
- Calvo-Flores Guzman, B., et al., 2018. The GABAergic system as a therapeutic target for Alzheimer's disease. *J. Neurochem.* 146, 649–669. <https://doi.org/10.1111/jnc.14345>.
- Calvo-Flores Guzman, B., et al., 2020a. Amyloid-Beta(1-42) -Induced increase in GABAergic tonic conductance in mouse hippocampal CA1 pyramidal cells. *Molecules* 25. <https://doi.org/10.3390/molecules25030693>.
- Calvo-Flores Guzman, B., et al., 2020b. The interplay between beta-amyloid 1-42 (A $\beta$ 1-42)-induced hippocampal inflammatory response, p-tau, vascular pathology, and their synergistic contributions to neuronal death and behavioral deficits. *Front. Mol. Neurosci.* 13, 522073. <https://doi.org/10.3389/fnmol.2020.552073>.
- Carello-Collar, G., et al., 2023. The GABAergic system in Alzheimer's disease: a systematic review with meta-analysis. *Mol. Psychiatr.* <https://doi.org/10.1038/s41380-023-02140-w>.
- Chambers, M.S., et al., 2004. An orally bioavailable, functionally selective inverse agonist at the benzodiazepine site of GABA(A) receptors with cognition enhancing properties. *J. Med. Chem.* 47, 5829–5832. <https://doi.org/10.1021/jm040863t>.
- Choi, G.-Y., et al., 2023. Naringin enhances long-term potentiation and recovers learning and memory deficits of amyloid-beta induced Alzheimer's disease-like behavioral rat model. *Neurotoxicology* 95, 35–45. <https://doi.org/10.1016/j.neuro.2022.12.007>.
- Collinson, N., et al., 2002. Enhanced learning and memory and altered GABAergic synaptic transmission in mice lacking the alpha 5 subunit of the GABA(A) receptor. *J. Neurosci.* 22, 5572–5580. <https://doi.org/10.1523/jneurosci.22-13-05572.2002>.
- Collinson, N., Atack, J.R., Loughton, P., Dawson, G.R., Stephens, D.N., 2006. An inverse agonist selective for alpha5 subunit-containing GABA(A) receptors improves encoding and recall but not consolidation in the morris water maze. *Psychopharmacology (Berl)* 188, 619–628. <https://doi.org/10.1007/s00213-006-0361-z>.
- Crestani, F., et al., 2002. Trace fear conditioning involves hippocampal alpha5 GABA(A) receptors. *Proc. Natl. Acad. Sci. U. S. A.* 99, 8980–8985. <https://doi.org/10.1073/pnas.142288699>.
- Davenport, C.M., et al., 2021. Relocation of an extrasynaptic GABA(A) receptor to inhibitory synapses freezes excitatory synaptic strength and preserves memory. *Neuron* 109, 123–134.e124. <https://doi.org/10.1016/j.neuron.2020.09.037>.
- Dawson, G.R., et al., 2006. An inverse agonist selective for alpha5 subunit-containing GABA(A) receptors enhances cognition. *J. Pharmacol. Exp. Therapeut.* 316, 1335–1345. <https://doi.org/10.1124/jpet.105.092320>.
- Duchon, A., et al., 2020. Long-lasting correction of in vivo LTP and cognitive deficits of mice modelling Down syndrome with an  $\alpha 5$ -selective GABA(A) inverse agonist. *Br. J. Pharmacol.* 177, 1106–1118. <https://doi.org/10.1111/bph.14903>.
- Eng, W., et al., 2010. Occupancy of human brain GABA(A) receptors by the novel  $\alpha 5$  subtype-selective benzodiazepine site inverse agonist  $\alpha 5A$  as measured using [ $^{11}C$ ] flumazenil PET imaging. *Neuropharmacology* 59, 635–639. <https://doi.org/10.1016/j.neuropharm.2010.07.024>.
- Francis, P.T., 2005. The interplay of neurotransmitters in Alzheimer's disease. *CNS Spectr.* 10, 6–9. <https://doi.org/10.1017/S1092852900014164>.
- Gillespie, A.K., et al., 2016. Apolipoprotein E4 causes age-dependent disruption of slow gamma oscillations during hippocampal sharp-wave ripples. *Neuron* 90, 740–751. <https://doi.org/10.1016/j.neuron.2016.04.009>.
- Giovannetti, E.A., et al., 2018. Restoring memory by optogenetic synchronization of hippocampal oscillations in an Alzheimer's disease mouse model. *bioRxiv*, 363820. <https://doi.org/10.1101/363820>.
- Glykys, J., Mody, I., 2006. Hippocampal network hyperactivity after selective reduction of tonic inhibition in GABA(A) receptor  $\alpha 5$  subunit-deficient mice. *J. Neurophysiol.* 95, 2796–2807. <https://doi.org/10.1152/jn.01122.2005>.
- Goeldner, C., et al., 2022. A randomized, double-blind, placebo-controlled phase II trial to explore the effects of a GABA(A)- $\alpha 5$  NAM (basmisnil) on intellectual disability associated with Down syndrome. *J. Neurodev. Disord.* 14, 10. <https://doi.org/10.1186/s11689-022-09418-0>.
- Govindpani, K., et al., 2017. Towards a better understanding of GABAergic remodeling in Alzheimer's disease. *Int. J. Mol. Sci.* 18. <https://doi.org/10.3390/ijms18081813>.
- Gulyás, A.I., Megias, M., Emri, Z., Freund, T.F., 1999. Total number and ratio of excitatory and inhibitory synapses converging onto single interneurons of different types in the CA1 area of the rat hippocampus. *J. Neurosci.* 19, 10082–10097. <https://doi.org/10.1523/jneurosci.19-22-10082.1999>.
- Harkany, T., et al., 2000. beta-amyloid neurotoxicity is mediated by a glutamate-triggered excitotoxic cascade in rat nucleus basalis. *Eur. J. Neurosci.* 12, 2735–2745. <https://doi.org/10.1046/j.1460-9568.2000.00164.x>.
- Hipp, J.F., et al., 2021. Basmisnil, a highly selective GABA(A)- $\alpha 5$  negative allosteric modulator: preclinical pharmacology and demonstration of functional target engagement in man. *Sci. Rep.* 11, 7700. <https://doi.org/10.1038/s41598-021-87307-7>.
- Howell, O., Atack, J.R., Dewar, D., McKernan, R.M., Sur, C., 2000. Density and pharmacology of  $\alpha 5$  subunit-containing GABA(A) receptors are preserved in hippocampus of Alzheimer's disease patients. *Neuroscience* 98, 669–675. [https://doi.org/10.1016/S0306-4522\(00\)00163-9](https://doi.org/10.1016/S0306-4522(00)00163-9).
- Iaccarino, H.F., et al., 2016. Gamma frequency entrainment attenuates amyloid load and modifies microglia. *Nature* 540, 230–235. <https://doi.org/10.1038/nature20587>.
- Jiménez-Balado, J., Eich, T.S., 2021. GABAergic dysfunction, neural network hyperactivity and memory impairments in human aging and Alzheimer's disease. *Semin. Cell Dev. Biol.* 116, 146–159. <https://doi.org/10.1016/j.semcdb.2021.01.005>.
- Jo, S., et al., 2014. GABA from reactive astrocytes impairs memory in mouse models of Alzheimer's disease. *Nat. Med.* 20, 886–896. <https://doi.org/10.1038/nm.3639>.
- Kammel, L.G., Wei, W., Jami, S.A., Voskuhl, R.R., O'Dell, T.J., 2018. Enhanced GABAergic tonic inhibition reduces intrinsic excitability of hippocampal CA1 pyramidal cells in experimental autoimmune encephalomyelitis. *Neuroscience* 395, 89–100. <https://doi.org/10.1016/j.neuroscience.2018.11.003>.
- Kapust, R.B., Waugh, D.S., 1999. Escherichia coli maltose-binding protein is uncommonly effective at promoting the solubility of polypeptides to which it is fused. *Protein Sci.* 8, 1668–1674. <https://doi.org/10.1110/ps.8.8.1668>.

- Kawaharada, S., et al., 2018. ONO-8590580, a novel GABA(A) $\alpha$ 5 negative allosteric modulator enhances long-term potentiation and improves cognitive deficits in preclinical models. *J. Pharmacol. Exp. Therapeut.* 366, 58–65. <https://doi.org/10.1124/jpet.117.247627>.
- Koh, J.-y., Choi, D.W., 1991. Selective blockade of non-NMDA receptors does not block rapidly triggered glutamate-induced neuronal death. *Brain Res.* 548, 318–321. [https://doi.org/10.1016/0006-8993\(91\)91140-V](https://doi.org/10.1016/0006-8993(91)91140-V).
- Koh, M.T., Rosenzweig-Lipson, S., Gallagher, M., 2013. Selective GABA(A)  $\alpha$ 5 positive allosteric modulators improve cognitive function in aged rats with memory impairment. *Neuropharmacology* 64, 145–152. <https://doi.org/10.1016/j.neuropharm.2012.06.023>.
- Kwakowsky, A., et al., 2016a. Treatment of beta amyloid 1–42 ( $A\beta$ 1–42)-induced basal forebrain cholinergic damage by a non-classical estrogen signaling activator in vivo. *Sci. Rep.* 6, 21101. <https://doi.org/10.1038/srep21101>.
- Kwakowsky, A., et al., 2016b. Treatment of beta amyloid 1–42 ( $A\beta$ (1–42))-induced basal forebrain cholinergic damage by a non-classical estrogen signaling activator in vivo. *Sci. Rep.* 6, 21101. <https://doi.org/10.1038/srep21101>.
- Kwakowsky, A., et al., 2018a. GABA(A) receptor subunit expression changes in the human Alzheimer's disease hippocampus, subiculum, entorhinal cortex and superior temporal gyrus. *J. Neurochem.* 145, 374–392. <https://doi.org/10.1111/jnc.14325>.
- Kwakowsky, A., Calvo-Flores Guzman, B., Govindpani, K., Waldvogel, H.J., Faull, R.L., 2018b. Gamma-aminobutyric acid A receptors in Alzheimer's disease: highly localized remodeling of a complex and diverse signaling pathway. *Neural Regen. Res.* 13, 1362–1363. <https://doi.org/10.4103/1673-5374.235240>.
- Kwakowsky, A., Waldvogel, H.J., Faull, R.L.M., 2021. Therapeutic potential of alpha 5 subunit containing GABA(A) receptors in Alzheimer's disease. *Neural Regen. Res.* 16, 1550–1551. <https://doi.org/10.4103/1673-5374.300987>.
- Lee, V., Maguire, J., 2014. The impact of tonic GABA receptor-mediated inhibition on neuronal excitability varies across brain region and cell type. *Front. Neural Circ.* 8. <https://doi.org/10.3389/fncir.2014.00003>.
- Li, Y., et al., 2016. Implications of GABAergic neurotransmission in Alzheimer's disease. *Front. Aging Neurosci.* 8, 31. <https://doi.org/10.3389/fnagi.2016.00031>.
- Liu, Y., et al., 2020. Muscone ameliorates synaptic dysfunction and cognitive deficits in APP/PS1 mice. *J. Alzheimers Dis.* 76, 491–504. <https://doi.org/10.3233/JAD-200188>.
- Madl, J.E., Royer, S.M., 2000. Glutamate dependence of GABA levels in neurons of hypoxic and hypoglycemic rat hippocampal slices. *Neuroscience* 96, 657–664.
- Mann, E.O., Paulsen, O., 2007. Role of GABAergic inhibition in hippocampal network oscillations. *Trends Neurosci.* 30, 343–349. <https://doi.org/10.1016/j.tins.2007.05.003>.
- Mann, E.O., Radcliffe, C.A., Paulsen, O., 2005. Hippocampal gamma-frequency oscillations: from interneurons to pyramidal cells, and back. *J. Physiol.* 562, 55–63. <https://doi.org/10.1113/jphysiol.2004.078758>.
- Manzo, M.A., et al., 2021. Inhibition of a tonic inhibitory conductance in mouse hippocampal neurons by negative allosteric modulators of  $\alpha$ 5 subunit-containing  $\gamma$ -aminobutyric acid type A receptors: implications for treating cognitive deficits. *Br. J. Anaesth.* 126, 674–683. <https://doi.org/10.1016/j.bja.2020.11.032>.
- Martin, L.J., Oh, G.H., Orser, B.A., 2009. Etomidate targets alpha5 gamma-aminobutyric acid subtype A receptors to regulate synaptic plasticity and memory blockade. *Anesthesiology* 111, 1025–1035. <https://doi.org/10.1097/ALN.0b013e3181bbc961>.
- Milior, G., et al., 2016. Electrophysiological properties of CA1 pyramidal neurons along the longitudinal axis of the mouse hippocampus. *Sci. Rep.* 6, 38242. <https://doi.org/10.1038/srep38242>.
- Mucke, L., 2018. PL-01-02: aberrant network activity in ALZHEIMER'S disease: preclinical investigation to clinical trials. *Alzheimer's Dement.* 14, P210. <https://doi.org/10.1016/j.jalz.2018.06.2324>.
- Nutt, D.J., Besson, M., Wilson, S.J., Dawson, G.R., Lingford-Hughes, A.R., 2007. Blockade of alcohol's amnesic activity in humans by an alpha5 subtype benzodiazepine receptor inverse agonist. *Neuropharmacology* 53, 810–820. <https://doi.org/10.1016/j.neuropharm.2007.08.008>.
- Nuwer, J.L., Povysheva, N., Jacob, T.C., 2023. Long-term  $\alpha$ 5 GABA A receptor negative allosteric modulator treatment reduces NMDAR-mediated neuronal excitation and maintains basal neuronal inhibition. *Neuropharmacology* 237, 109587. <https://doi.org/10.1016/j.neuropharm.2023.109587>.
- Olsen, R.W., Sieghart, W., 2009. GABA A receptors: subtypes provide diversity of function and pharmacology. *Neuropharmacology* 56, 141–148. <https://doi.org/10.1016/j.neuropharm.2008.07.045>.
- O'Connell, A., Quinlan, L., Kwakowsky, A., 2024.  $\beta$ -amyloid's neurotoxic mechanisms as defined by in vitro microelectrode arrays: a review. *Pharmacol. Res.* 209, 107436. <https://doi.org/10.1016/j.phrs.2024.107436>.
- Palop, J.J., Mucke, L., 2016. Network abnormalities and interneuron dysfunction in Alzheimer disease. *Nat. Rev. Neurosci.* 17, 777–792. <https://doi.org/10.1038/nrn.2016.141>.
- Palop, J.J., et al., 2007. Aberrant excitatory neuronal activity and compensatory remodeling of inhibitory hippocampal circuits in mouse models of Alzheimer's disease. *Neuron* 55, 697–711. <https://doi.org/10.1016/j.neuron.2007.07.025>.
- Paulsen, O., Moser, E.I., 1998. A model of hippocampal memory encoding and retrieval: GABAergic control of synaptic plasticity. *Trends Neurosci.* 21, 273–278. [https://doi.org/10.1016/s0166-2236\(97\)01205-8](https://doi.org/10.1016/s0166-2236(97)01205-8).
- Petrache, A.L., et al., 2020. Selective modulation of  $\alpha$ 5 GABAA receptors exacerbates aberrant inhibition at key hippocampal neuronal circuits in APP mouse model of Alzheimer's disease. *Front. Cell. Neurosci.* 14. <https://doi.org/10.3389/fncel.2020.568194>, 2020.
- Ratner, M.H., et al., 2021. Prodromal dysfunction of  $\alpha$ 5GABA-A receptor modulated hippocampal ripples occurs prior to neurodegeneration in the TgF344-AD rat model of Alzheimer's disease. *Heliyon* 7, e07895. <https://doi.org/10.1016/j.heliyon.2021.e07895>.
- Rissman, R.A., Mobley, W.C., 2011. Implications for treatment: GABAA receptors in aging, Down syndrome and Alzheimer's disease. *J. Neurochem.* 117, 613–622. <https://doi.org/10.1111/j.1471-4159.2011.07237.x>.
- Rissman, R.A., De Blas, A.L., Armstrong, D.M., 2007. GABA(A) receptors in aging and Alzheimer's disease. *J. Neurochem.* 103, 1285–1292. <https://doi.org/10.1111/j.1471-4159.2007.04832.x>.
- Sánchez-Rodríguez, I., et al., 2017. Activation of G-protein-gated inwardly rectifying potassium (Kir3/GirK) channels rescues hippocampal functions in a mouse model of early amyloid- $\beta$  pathology. *Sci. Rep.* 7, 14658. <https://doi.org/10.1038/s41598-017-15306-8>.
- Sánchez-Rodríguez, I., Gruart, A., Delgado-García, J.M., Jiménez-Díaz, L., Navarro-López, J.D., 2019. Role of KirK channels in long-term potentiation of synaptic inhibition in an in vivo mouse model of early Amyloid- $\beta$  pathology. *Int. J. Mol. Sci.* 20. <https://doi.org/10.3390/ijms20051168>.
- Song, I., Savtchenko, L., Semyanov, A., 2011. Tonic excitation or inhibition is set by GABA(A) conductance in hippocampal interneurons. *Nat. Commun.* 2, 376. <https://doi.org/10.1038/ncomms1377>.
- Soria Lopez, J.A., González, H.M., Léger, G.C., 2019. Alzheimer's disease. *Handb. Clin. Neurol.* 167, 231–255. <https://doi.org/10.1016/b978-0-12-804766-8.00013-3>.
- Tamagnini, F., Scullion, S., Brown, J.T., Randall, A.D., 2015. Intrinsic excitability changes induced by acute treatment of hippocampal CA1 pyramidal neurons with exogenous amyloid  $\beta$  peptide. *Hippocampus* 25, 786–797. <https://doi.org/10.1002/hipo.22403>.
- Towers, S.K., et al., 2004. Alpha 5 subunit-containing GABAA receptors affect the dynamic range of mouse hippocampal kainate-induced gamma frequency oscillations in vitro. *J. Physiol.* 559, 721–728. <https://doi.org/10.1113/jphysiol.2004.071191>.
- Varga, E., et al., 2014. Abeta(1-42) enhances neuronal excitability in the CA1 via NR2B subunit-containing NMDA receptors. *Neural Plast.* 2014, 584314. <https://doi.org/10.1155/2014/584314>.
- Verret, L., et al., 2012. Inhibitory interneuron deficit links altered network activity and cognitive dysfunction in Alzheimer model. *Cell* 149, 708–721. <https://doi.org/10.1016/j.cell.2012.02.046>.
- Vinnakota, C., et al., 2020. An  $\alpha$ 5 GABAA receptor inverse agonist, 5IA, attenuates amyloid beta-induced neuronal death in mouse hippocampal cultures. *Int. J. Mol. Sci.* 21. <https://doi.org/10.3390/ijms21093284>.
- Wang, Y., et al., 2020. Oligomer  $\beta$ -amyloid induces hyperactivation of ras to impede NMDA receptor-dependent long-term potentiation in hippocampal CA1 of mice. *Front. Pharmacol.* 11, 595360. <https://doi.org/10.3389/fphar.2020.595360>.
- World health organisation, WHO, 2020.
- Wu, J., Anwyl, R., Rowan, M.J., 1995. beta-Amyloid selectively augments NMDA receptor-mediated synaptic transmission in rat hippocampus. *Neuroreport* 6, 2409–2413. <https://doi.org/10.1097/00001756-199511270-00031>.
- Wu, Z., Guo, Z., Gearing, M., Chen, G., 2014a. Tonic inhibition in dentate gyrus impairs long-term potentiation and memory in an Alzheimer's [corrected] disease model. *Nat. Commun.* 5, 4159. <https://doi.org/10.1038/ncomms5159>.
- Wu, Z., Guo, Z., Gearing, M., Chen, G., 2014b. Tonic inhibition in dentate gyrus impairs long-term potentiation and memory in an Alzheimer's disease model. *Nat. Commun.* 5. <https://doi.org/10.1038/ncomms5159>.
- Xu, N.Z., et al., 2018. Negative allosteric modulation of alpha 5-containing GABA(A) receptors engenders antidepressant-like effects and selectively prevents age-associated hyperactivity in tau-depositing mice. *Psychopharmacology (Berl)* 235, 1151–1161. <https://doi.org/10.1007/s00213-018-4832-9>.
- Xu, Y., Zhao, M., Han, Y., Zhang, H., 2020. GABAergic inhibitory interneuron deficits in Alzheimer's disease: implications for treatment. *Front. Neurosci.* 14. <https://doi.org/10.3389/fnins.2020.00660>.
- Yeung, J.H.Y., et al., 2020. The acute effects of Amyloid-Beta1–42 on glutamatergic receptor and transporter expression in the mouse hippocampus. *Front. Neurosci.* 13. <https://doi.org/10.3389/fnins.2019.01427>.
- Yuan, C., et al., 2021. A multi-dosing regimen to enhance the spatial memory of normal rats with  $\alpha$ 5-containing GABA(A) receptor negative allosteric modulator L-655,708. *Psychopharmacology (Berl)* 238, 3375–3389. <https://doi.org/10.1007/s00213-021-05951-3>.